

APPROVED FOR RELEASE: 2007/02/08: CIA-RDP82-00850R000100090041-6

25 SEPTEMBER 1979

» AND :
(FOUO 5/79)

1 OF 1

FOR OFFICIAL USE ONLY

JPRS L/8682

25 September 1979

USSR Report

GEOPHYSICS, ASTRONOMY AND SPACE

(FOUO 5/79)

FBIS FOREIGN BROADCAST INFORMATION SERVICE

FOR OFFICIAL USE ONLY

NOTE

JPRS publications contain information primarily from foreign newspapers, periodicals and books, but also from news agency transmissions and broadcasts. Materials from foreign-language sources are translated; those from English-language sources are transcribed or reprinted, with the original phrasing and other characteristics retained.

Headlines, editorial reports, and material enclosed in brackets [] are supplied by JPRS. Processing indicators such as [Text] or [Excerpt] in the first line of each item, or following the last line of a brief, indicate how the original information was processed. Where no processing indicator is given, the information was summarized or extracted.

Unfamiliar names rendered phonetically or transliterated are enclosed in parentheses. Words or names preceded by a question mark and enclosed in parentheses were not clear in the original but have been supplied as appropriate in context. Other unattributed parenthetical notes within the body of an item originate with the source. Times within items are as given by source.

The contents of this publication in no way represent the policies, views or attitudes of the U.S. Government.

For further information on report content
call (703) 351-2938 (economic); 3468
(political, sociological, military); 2726
(life sciences); 2725 (physical sciences).

COPYRIGHT LAWS AND REGULATIONS GOVERNING OWNERSHIP OF
MATERIALS REPRODUCED HEREIN REQUIRE THAT DISSEMINATION
OF THIS PUBLICATION BE RESTRICTED FOR OFFICIAL USE ONLY.

FOR OFFICIAL USE ONLY

JPRS L/8682

25 September 1979

USSR REPORT
GEOPHYSICS, ASTRONOMY AND SPACE
(FOUO 5/79)

This serial publication contains articles, abstracts of articles and news items from USSR scientific and technical journals on the specific subjects reflected in the table of contents.

Photoduplications of foreign-language sources may be obtained from the Photoduplication Service, Library of Congress, Washington, D. C. 20540. Requests should provide adequate identification both as to the source and the individual article(s) desired.

	CONTENTS	PAGE
I.	OCEANOGRAPHY.....	1
	Translations.....	1
	Synoptic Eddies in the Open Ocean -- A New Discovery in Oceanology.....	1
	Study of Deep Faults.....	12
	Geomagnetic Field Disturbances Created by Sea Currents.....	23
	Electromagnetic Field of Sea Waves in an Electrically Stratified Sea.....	32
	Systemic Principles for Analysis of Ocean Observations...	41

- a - [III - USSR - 21J S&T FOUO]

FOR OFFICIAL USE ONLY

FOR OFFICIAL USE ONLY

I. OCEANOGRAPHY

Translations

UDC 551.46

SYNOPTIC EDDIES IN THE OPEN OCEAN -- A NEW DISCOVERY IN OCEANOLOGY

Moscow VESTNIK AKADEMII NAUK SSSR in Russian No 6, 1979 pp 43-51

[Article by Doctor of Physical and Mathematical Sciences M. N. Koshlyakov]

[Text] By the late 1950's-early 1960's oceanologists had a fair general idea concerning so-called macroscale circulation of ocean waters, that is, about the system of mean (in time) ocean currents, from which disturbances with periods less than a year are excluded. This idea was based primarily on indirect data obtained by means of an analysis of the distributions of temperature, salinity and dissolved oxygen in the world ocean and by means of computations of macroscale currents on the basis of the density distribution of ocean water. The links in such a macroscale circulation in the upper layer (with a thickness of about one kilometer) in the North Atlantic are, for example, the Gulf Stream, the North Atlantic Current and the North Trades Current (Fig. 1).

With respect to disturbances of mean circulation, by the late 1950's there had been a fairly good study of one extremely specific type of such disturbances -- the so-called frontal eddies of the Gulf Stream and Kuroshio, forming as a result of the development and subsequent cutoff of meanders (wavelike curvatures) of strong and narrow ocean currents (Fig. 2). [In this article we do not examine relatively short-period (not more than several days) disturbances of ocean circulation (tidal, inertial currents, internal gravitational waves.) The Gulf Stream and Kuroshio, like other links in macroscale ocean circulation, are primarily geostrophic currents, that is, those in whose field the horizontal pressure gradient is evened out by Coriolis force, as a result of which the current is directed along the isobars at any depth. Moreover, the dependence of pressure on density, and density on temperature leads to a rough coincidence, at individual horizons, of the current streamlines and isotherms. In the northern hemisphere to the right of the current there is usually warmer water, and to the left -- colder water (see Fig. 2). The great velocities of the Gulf Stream and Kuroshio and their relatively small width (several tens of kilometers) are responsible for the exceptional sharpness of the temperature drop across the current, which gives a frontal character to these currents.

FOR OFFICIAL USE ONLY

FOR OFFICIAL USE ONLY

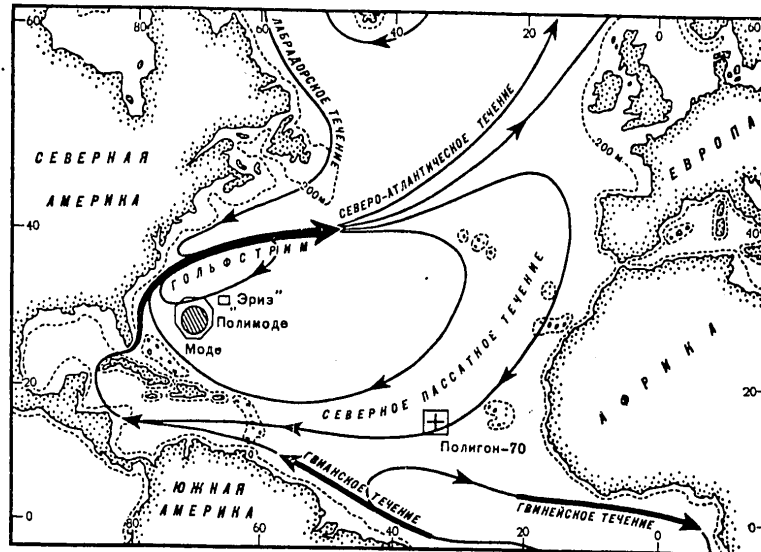


Fig. 1. Map of macroscale currents in the upper layer of the North Atlantic. Particularly strong currents are denoted by thick arrows. The characteristic velocity of the Gulf Stream and other particularly strong currents is $1 \text{ cm} \cdot \text{sec}^{-1}$, in the open ocean -- $1.10 \text{ cm} \cdot \text{sec}^{-1}$, special symbols denote the sites where several oceanographic expeditions mentioned in the article were carried out.

It is evident that the properties of geostrophicity and frontality are also retained for the eddies of the Gulf Stream and Kuroshio because they simply represent the cut-off and closing parts of the frontal currents. Within the cyclones of the Gulf Stream and Kuroshio, penetrating into the region of the warm ocean to the south of the currents, the water is cold, whereas within the anticyclones, penetrating into the cold region to the north of the currents, the water is warm. Observations of recent years have indicated, for example, that about five pairs of cyclones and anticyclones are formed annually in the Gulf Stream field. The especially well-developed cyclones of the Gulf Stream have a diameter of about 200 km and penetrate several kilometers into the depth of the ocean. The difference in depths of isothermal surfaces between the centers of these eddies and their periphery can attain 700 m and the velocity of rotation of water in their upper part is 2 m/sec or even more.

Gulf Stream cyclones drift for the most part to the southwest (with a velocity of 3-5 km/day) as some individual formations surrounded by the quiet ocean. Observations show that in any case in the upper layer of the ocean

FOR OFFICIAL USE ONLY

FOR OFFICIAL USE ONLY

(to a depth of 700-1,000 m) this drift has a transfer, not a wave character: the eddy "drags along" the water mass constituting its inner part. Individual Gulf Stream cyclones have a lifetime as much as two years or more, gradually losing their energy as a result of mixing with the surrounding water, and can deviate a distance of more than 1,000 km from the Gulf Stream.

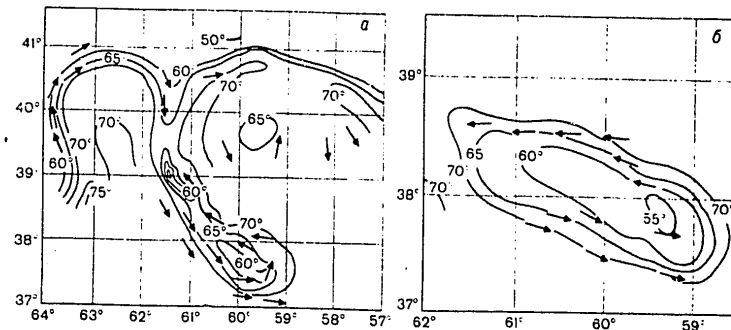


Fig. 2. Formation of cold cyclonic (rotation of water counterclockwise) eddy of the Gulf Stream (according to F. Fuglister and L. Worthington, 1951). a) data for 17 January 1950, b) data for 21 January 1950; the curves represent the isotherms at a depth of 200 m; water temperature in degrees F; the arrows indicate the direction of the current in the surface layer of the ocean.

The frontal eddies of the Gulf Stream and Kuroshio are observed in two relatively limited regions of the world ocean. What is the situation in its remaining parts? Are there disturbances of macroscale circulation there which with respect to spatial scales, periods and amplitudes are comparable with frontal eddies? By the 1950's the most popular point of view among oceanologists was that the system of macroscale currents in the main part of the world ocean, especially in its depths, is more or less stable, and the mean current velocity and direction at a stipulated point in the ocean (averaged for several days) must not, usually, differ very significantly from the mean seasonal or even mean climatic values.

However, in the late 1950's-early 1960's, when oceanologists began to obtain data from long-term measurements of the temperature, salinity and density of ocean water at some fixed points in the world ocean (for the most part these were data from so-called weather ships), it became clear that ocean depths are characterized by well-expressed variations of these oceanographic parameters with periods of about several months. Oceanologists also gave much attention to the results of measurements of deep ocean currents of freely drifting deep buoys made by the British oceanologist J. Swallow during the period 1959-1960 from the ship "Eris" (see Fig. 1) to the southwest of the Bermudas, where the velocity of the mean climatic current does not exceed $1-2 \text{ cm}\cdot\text{sec}^{-1}$. These measurements indicated that at depths of 2 and 4 km there are nonstationary currents with a period of about three months and velocities up to $40 \text{ cm}\cdot\text{sec}^{-1}$.

FOR OFFICIAL USE ONLY

FOR OFFICIAL USE ONLY

Thus, by the 1960's data had been accumulated on the presence of extremely significant nonstationary long-period water movements in different regions of the world ocean. However, fundamental problems remained unclarified: how typical are these movements for the ocean as a whole? In what way are they similar to the eddies of the Gulf Stream and Kuroshio and how do they differ from them? Do they constitute large-scale ocean turbulence or are they movements of a wave type? Do they fill the ocean completely or do they constitute quasi-isolated disturbances? What is their spatial scale and how is it related to the time scale? What is their energy and where does it come from? It became obvious that there was a need for a special expedition for obtaining at least partial answers to these questions. The "Polygon-70" experiment became such a measure.

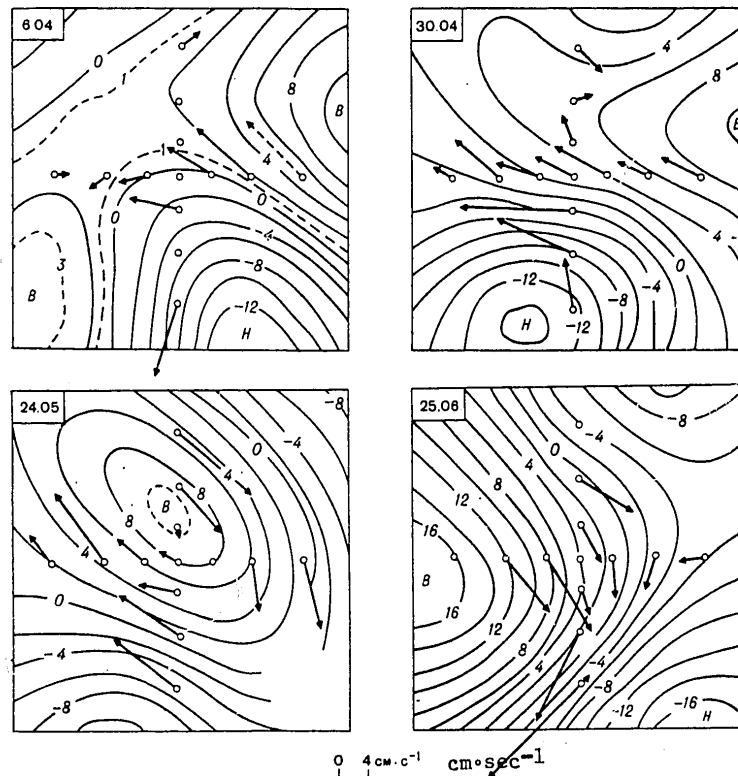


Fig. 3. Evolution of current pattern at depth of 300 m determined using data from "Polygon-70" experiment (1970). It is clear that the system of synoptic eddies is displaced to the west. Center of region -- $16^{\circ}30'N$, $33^{\circ}30'W$; side of square -- 280 km; small circles -- locations of buoy stations; arrows -- current velocity vectors; dashed arrows -- velocity vectors obtained by interpolation in depth or time; curves -- streamlines computed from velocity vectors using special interpolation program; the figures on the curves represent disturbances of the stream function in $10^7 \text{ cm}^2 \cdot \text{sec}^{-1}$; B -- high-pressure centers; H -- low-pressure centers; velocity scale at the bottom.

FOR OFFICIAL USE ONLY

FOR OFFICIAL USE ONLY

"Polygon-70" was the next in a series of Soviet oceanographic experiments organized and carried out beginning in the mid-1950's in different parts of the world ocean on the initiative of the outstanding Soviet oceanologist Professor V. B. Shtokman. The purpose of all these experiments was a study of the variability of ocean currents. The measurement base was polygons with anchored buoy stations outfitted with current meters. The buoy station is an anchor-cable-buoy station with several automatic current meters, attached to the cable at different horizons. Having the results of prolonged current measurements at several buoy stations, arranged in a definite way relative to one another, oceanologists are obtaining information on the spatial structure and temporal variability of the field of currents in the investigated region of the ocean.

The "Polygon-70" experiment was carried out by the Institute of Oceanology imeni P. P. Shirshov USSR Academy of Sciences and other Soviet oceanographic institutes under the scientific direction of Academician L. M. Brekhovskikh in the spring and summer of 1970, in the tropical part of the North Atlantic, in the region of the North Trades Current (see Fig. 1). Fundamental measurements of currents were made at 17 buoy stations arranged in a cross, operating in the ocean from late February to early September 1970; at each station the measurements were made at 10 horizons in the layer from the ocean surface to a depth of 1,500 m.

The principal result of the "Polygon-70" experiment was the discovery and surveying of several powerful eddylike disturbances in the current velocity field moving through the observation region (Fig. 3). These disturbances were so clearly expressed that they completely masked the large-scale North Trades Current. Like the frontal eddies of the Gulf Stream, they had a diameter of about 200 km, had a geostrophic character and penetrated a considerable depth into the ocean. The velocity of their movement to the west was about 5 km/day and the velocity of the orbital (rotational) movement of the water in their field attained $30-40 \text{ cm}\cdot\text{sec}^{-1}$ at depths of 100-800 m. In contrast, however, from the frontal eddies the "Polygon-70" eddies in their totality constituted a continuous field of cyclones and anticyclones arranged in an approximately checkerboard fashion. Two adjacent eddies had a common region of maximum current velocity with which another fundamental property of the "Polygon-70" eddies was associated, this fundamentally distinguishing them from the frontal eddies: their movement (to the west) had a primarily wavelike, not advective (transfer) character.

In other words, the "Polygon-70" eddies, in all probability are unusual quasi-horizontal waves, in whose field the particles move in orbits close to closed. The translational movement of the eddy (in the considered case — to the west) occurs due to the phase shifts of quasihorizontal orbital motion of adjacent water particles. An analysis of the relationship of the horizontal dimensions of "Polygon-70" eddies and the velocity of their movement to the west indicated that this relationship is precisely that which should be characteristic for so-called baroclinic Rossby waves -- wave movements in a

FOR OFFICIAL USE ONLY

FOR OFFICIAL USE ONLY

density-stratified ocean, whose kinematics and local dynamics are determined by the joint effect of the earth's sphericity and rotation. A simple hydrodynamic analysis of movement in the field of Rossby waves shows that without fail they must move in a westerly direction.

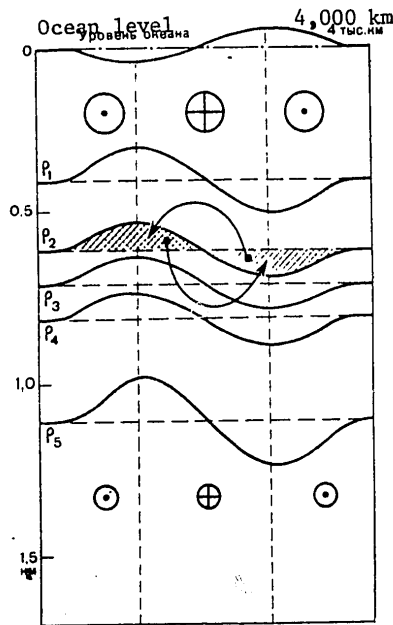


Fig. 4. Diagram of distribution of ocean level, water density and current velocity in vertical section through system of macroscale geostrophic currents in the northern hemisphere. The circles with the crosses are for currents moving in the plane of the figure; the circles with the dots are for currents moving from the plane of the figure; a larger circle represents a greater current velocity; the ρ curves represent individual isopycnal lines (water density increases with depth); the shaded regions and the arrows represent the setting free of APELSC with the straightening of isopycnal lines (the heavier water in this case subsides, the lighter water rises); the real drop in ocean level across the current is about a meter; the drop in the heights of isopycnal surfaces is several hundreds of meters; the typical current velocity at the ocean surface is $5-10 \text{ cm}\cdot\text{sec}^{-1}$, in depth -- $0.5-1 \text{ cm}\cdot\text{sec}^{-1}$.

The eddy movements discovered during the time of the "Polygon-70" experiment have been given the name "synoptic eddies of the open ocean." Such a name is attributable to the physical analogy between these eddies and moving atmospheric cyclones and anticyclones, manifested in an identical

FOR OFFICIAL USE ONLY

FOR OFFICIAL USE ONLY

predominant mechanism of their generation (baroclinic instability of macro-scale circulation, a subject which will be discussed below), a similar physical nature (baroclinic Rossby waves) and quasigeostrophicity of movement.

The region of the "Polygon-70" expedition is typical for the open ocean in its remoteness from the shores and frontal regions and the relatively low velocities of the large-scale current. Therefore, immediately after obtaining the results from the experiment it was postulated that the pattern of synoptic eddies discovered in the polygon should also be typical for the open ocean. This assumption was completely confirmed by both new oceanic experiments, especially directed to an investigation of synoptic eddies in the open ocean and an analysis, from a new point of view, of data from some old oceanographic observations. Among the new experiments the most important was MODE-1 (Mid-Ocean Dynamical Experiment-1), carried out by American oceanologists in the spring of 1973 in the southwestern part of the Sargasso Sea and giving results which in essence are close to the "Polygon-70" results. In subsequent years, on expeditions and in an analysis of old data, synoptic eddies or their obvious traces were discovered in the equatorial zone of the Pacific Ocean, to the east and west of Australia, in the region of the Hawaiian Islands, in Drake Strait and in some other parts of the Antarctic Ocean, in the Arctic Basin, to the west of California, in the zone of the North Atlantic Current, to the southwest of the southern extremity of Africa and in a number of other regions in the world ocean.

An analysis of all the available data suggests that synoptic eddies are a typical (if not universal) property of the world ocean. The specific kinetic energy of eddies, varying in a very wide range, is usually greater in those regions of the ocean where there is a higher specific kinetic energy of large-scale currents and as a rule substantially (on the average by an order of magnitude) exceeds it. This latter circumstance directly leads us to the problem of the origin of synoptic eddies, or to the question of from whence they acquire their energy.

It can now be evidently considered clear that the principal mechanism of generation of eddies is the baroclinic instability of large-scale currents. In order to understand this mechanism from the point of view of energy exchange we recall, first of all, that the ocean is stably stratified, that is, the water density in it increases with depth, and second, the ocean is stratified stably, that is, the water density in it increases with depth, and second, as a result of the geostrophicity of macroscale ocean currents surfaces of equal density (temperature) in their field slope in the direction perpendicular to the direction of the current (Fig. 4). It follows from this that any large-scale current in the ocean has some "excess" of potential energy in comparison with such a state in the ocean when all the isopycnic surfaces (surfaces of equal density) are horizontal.

Simple estimates show that this excess of potential energy, called the available potential energy of large-scale currents (APELSC), as an average for the ocean exceeds their kinetic energy by at least two orders of magnitude.

FOR OFFICIAL USE ONLY

FOR OFFICIAL USE ONLY

The APELSC also is the energy reserve from which oceanic synoptic eddies draw their energy. In other words, the eddies seemingly tend to annihilate the slope of the isopycnic surfaces, whereas the vertical component of large-scale oceanic circulation maintains this slope. A hydrodynamic analysis of the movements of ocean water confirms this idea in the sense that it shows the actual instability of large-scale ocean currents -- arbitrary disturbances, imposed on the main current, grow and develop into synoptic eddies, which accomplish horizontal transport of mass (density) in the ocean. Incidentally, it follows from this that even with a relatively low energy of the eddies the transport form of movement in their displacement, although to a small degree, must nevertheless be present.

By the mid-1970's it became entirely obvious that a further fundamental advance in the investigation of synoptic eddies in the open ocean can be attained only by carrying out expeditionary work in the ocean, in its scale considerably exceeding "Polymode-70" or MODE-1. The very large Soviet-American experiment (to be more exact, the entire complex of oceanic experiments) POLYMODE, became a consequence of a clear understanding of this circumstance. The principal Soviet studies under the POLYMODE program were carried out in the central part of the Sargasso Sea during the period July 1977 through September 1978. This work was done with the participation of several Soviet oceanographic institutes, headed by the Institute of Oceanology imeni P. P. Shirshov USSR Academy of Sciences and nine scientific research ships. The scientific leader of the work was the director of the Institute of Oceanology Corresponding Member USSR Academy of Sciences A. S. Monin.

The basis for the Soviet work in the POLYMODE polygon was the annual measurements of currents and water temperatures carried out by the Institute of Oceanology in a system of buoy stations situated at the points of grid intersection of equilateral triangles with its center at 29°N, 70°W (Fig. 5). The distance between stations was 72 km and the diameter of the entire measurement region was about 300 km; current meters were situated at seven horizons in the layer from 100 to 1,400 m depth.

The results of the measurements were unusually interesting and important. The POLYMODE eddies with respect to some parameters are rather close to the "Polygon-70" eddies, occupied a considerable part of the ocean layer, had a diameter of 150-200 km and moved westward with a velocity of 2-6 km/day. At the same time, the high energy level of water movement in the field of POLYMODE eddies, exceeding the mean kinetic energy of "Polygon-70" eddies by a factor of approximately 3, led to the obtaining of fundamentally new information on a process of primary interest, nonlinear dynamic interaction between individual eddies. This process, very well expressed in the region where the experiment was carried out, led to such highly interesting effects, repeatedly registered during the POLYMODE period, as a marked redistribution of kinetic energy between individual parts of the eddy field, the formation of a quasi-isolated eddy or a quasi-isolated pair of eddies of different sign, the direct exchange of energies between adjacent eddies,

FOR OFFICIAL USE ONLY

FOR OFFICIAL USE ONLY

the disappearance of individual eddy centers and the appearance of new centers (see Fig. 5). As indicated by the measurements carried out during the POLYMODE period, the temperatures and salinities of ocean waters, the westward movement of the strongest POLYMODE eddies had (in any case, in the upper layer of the ocean) a partially advective (transfer) character. This means that with respect to some physical properties POLYMODE eddies can be regarded as intermediate formations between "Polygon-70" eddies and frontal eddies, although they "gravitate" toward "Polygon-70" eddies.

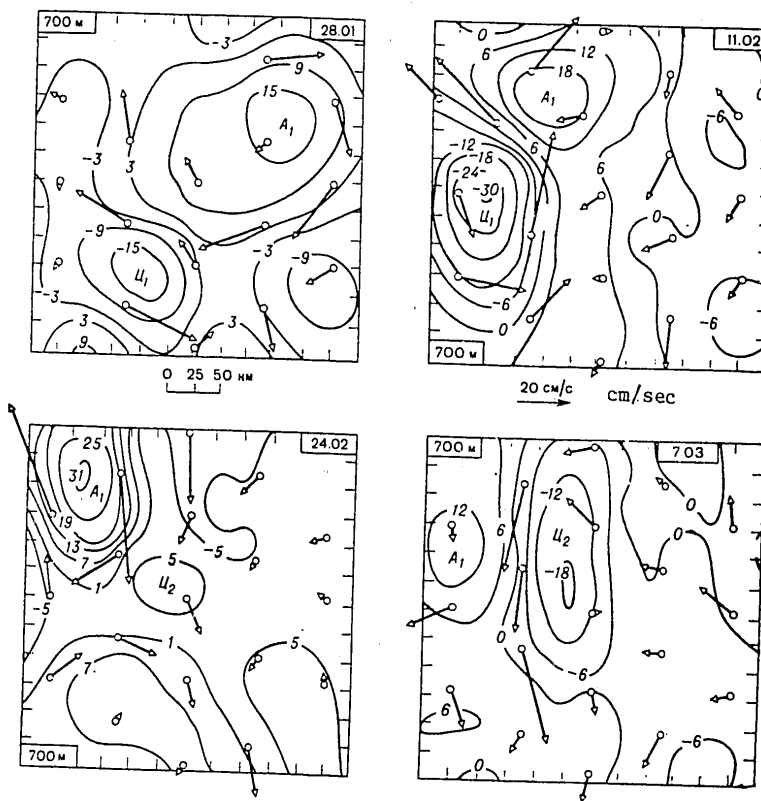


Fig. 5. Evolution of pattern of currents at a depth of 700 m according to POLYMODE data. Circles -- sites of buoy stations; arrows -- current velocity vectors; curves -- streamlines constructed on basis of velocity vectors using special interpolation program; the figures on the curves are the values of the stream function in $10^7 \text{ cm}^2 \cdot \text{sec}^{-1}$; A, U -- centers of individual anticyclones and cyclones; together with the general movement of eddies to the west it is easy to see a marked redistribution of energy between individual sectors of the eddy field, its concentration in individual quasi-isolated eddies, the disappearance of some eddies and the appearance of others.

FOR OFFICIAL USE ONLY

FOR OFFICIAL USE ONLY

From everything which has been said it should be clear that an extremely significant role is played by synoptic eddies in the processes of transfer and transformation of matter and energy in the ocean. Without a careful study of eddies it is impossible to have a thorough understanding of the physics of ocean circulation, and this means, the formulation of a physical model of macroscale interaction between the ocean and atmosphere sufficiently close to nature. Such a model, in turn, is completely necessary for creating reliable methods for the long-range forecasting of weather and climatic anomalies. As a result of the predominance of the kinetic energy of eddies over the kinetic energy of macroscale oceanic circulation the field of synoptic eddies is the real field of currents which acts on a vessel present in the ocean. Hence it is clear how important it is to investigate eddies for navigation in the ocean. The propagation of sound in the ocean is essentially dependent on the distribution of water density in it, which, as follows from what has been stated above, is determined to a great extent by the distribution of cyclonic and anticyclonic oceanic eddies.

We note, finally, that in the central parts of cyclonic eddies there is an upwelling of cold, deep ocean waters, whereas in the central parts of anticyclones, on the other hand, the subsidence of warm surface waters is observed. As is well known, the regions of upwelling of waters are characterized, in comparison with regions of subsidence, by a considerably greater biological productivity, and accordingly an investigation of eddies is also important for commercial biology.

Thus, an experimental and theoretical investigation of synoptic ocean eddies is becoming one of the most important directions in the development of physical oceanology in the upcoming years.

At a session of the Presidium USSR Academy of Sciences at which the scientific communication of M. N. Koshlyakov was presented, commentaries were made by Academicians G. I. Marchuk and L. M. Brekhovskikh.

G. I. Marchuk. In order to visualize more clearly the phenomenon discovered in the ocean, we will turn to atmospheric phenomena. In the atmosphere it is customary to observe fronts of cold and warm air. The air movements in these fronts are variable and nonuniform. It has been demonstrated by N. Ye. Kochin (and later by other researchers) that such movements are unstable. As a result of realization of instability rather stable formations arise -- eddies (cyclones and anticyclones). An atmospheric eddy lives approximately a week, gradually dissipating.

These same eddies have now been discovered in the ocean. Oceanic eddies live considerably longer (water density is far greater than air density) and play an extremely important role in its life. This discovery is of very great importance for explaining many macroscale phenomena in the ocean.

10

FOR OFFICIAL USE ONLY

FOR OFFICIAL USE ONLY

Now scientists are trying to answer the question as to why the earth's climate is changing, why it is that each year there is no repetition of the events which should be repeated in a well-determined, stable system. One of the explanations is evidently as follows. Somewhere, probably in the zone of the temperate latitudes, under the influence of some definite conditions, large temperature anomalies develop. These anomalies, which cannot be recognized from the surface, begin to migrate. They can migrate a month, a half-year, one-two years and unexpectedly emit great quantities of heat into the atmosphere.

A further study of the ocean (the first step has already been taken by the discovery of eddies) will make it possible to find the triggering mechanism which is responsible for interaction between the ocean and the atmosphere.

L. M. Brekhovskikh. Earlier the ocean was regarded as a stationary system. The currents in it were regarded as more or less constant; these currents were also plotted on maps. After the discovery of eddies we must now speak of "weather" in the ocean. We must study it as carefully as weather in the atmosphere because weather in the ocean also influences the weather of our planet in the most decisive way. It also exerts a great influence on processes transpiring in the ocean: on the life and distribution of nutrients, on the distribution of all kinds of wave disturbances. In short, a new page in ocean science, interesting and important, has been opened.

In conclusion, the Vice President of the USSR Academy of Sciences, Academician V. A. Kotel'nikov, thanked M. N. Koshlyakov for an interesting scientific communication.

COPYRIGHT: Izdatel'stvo "Nauka," "Vestnik Akademii nauk SSSR," 1979

[496-5303]

FOR OFFICIAL USE ONLY

FOR OFFICIAL USE ONLY

UDC 553.26

STUDY OF DEEP FAULTS

Moscow VESTNIK AKADEMII NAUK SSSR in Russian No 6, 1979 pp 77-85

[Article by Doctor of Physical and Mathematical Sciences Yu. P. Neprochnov]

[Text] Zones of deep, transformed faults are interesting because deep rocks of the earth's crust emerge here at the surface of the ocean floor and are accessible for direct geological investigations. Detailed geological studies in zones of transformed faults can substantially supplement ocean drilling, which makes it possible to penetrate into solid crustal rocks to only a small depth -- tens, in the best case, hundreds of meters. A comparison of geological and geophysical data will make it possible to obtain answers to important questions relating to the nature of magnetic and gravitational anomalies, on the composition of the main layers of the earth's crust detected in seismic investigations in the ocean.

Transformed faults were the principal feature studied by a multisided geological-geophysical expedition of the USSR Academy of Sciences aboard the scientific research vessel "Akademik Kurchatov" (24th voyage, December 1976-April 1977). The scientific program of the expedition provided for a comparative study of zones of major faults intersecting the Mid-Atlantic Ridge, the East Pacific Ocean Rise and adjacent basins.

The expedition was organized by the Institute of Oceanology imeni P. P. Shirshov USSR Academy of Sciences. Participating in the voyage were specialists of the Institute of Geography, Institute of Geology of Ore Deposits, Petrography, Mineralogy and Geochemistry, Institute of Terrestrial Magnetism, Ionosphere and Radio Wave Propagation, Geology Institute and Institute of Physics of the Earth imeni O. Yu. Shmidt USSR Academy of Sciences and also the USSR Geology Ministry and Moscow University.

The total extent of the expedition route, including studies in the polygon, was about 29,000 miles. In contrast to the preceding expeditions, on this voyage transformed faults were studied not only within the limits of the rift zones of the ridges, but also at a distance from them, in regions with a more ancient crust. Most of the work was done in five polygons each with an area of approximately 100 km², situated in the fault zones

FOR OFFICIAL USE ONLY

FOR OFFICIAL USE ONLY

Atlantis, Kane, Galapagos, Eltanin and an earlier unknown fault on the western slope of the East Pacific Ocean Rise (Fig. 1). In the polygons specialists first carried out a geophysical survey, including depth sounding, magnetometry, gravimetry and continuous seismic profiling (CSP) along a grid of runs with distances between them of 1-15 km. The results of the survey were processed on an electronic computer on shipboard and represented in the form of composite geophysical sections. This was followed by compilation of maps of bottom relief, magnetic and gravitational anomalies, thicknesses of the sedimentary cover and relief of the acoustic basement. Using data from a geophysical survey it was possible to determine the most favorable sectors for the dredging of bedrock, sampling of bottom sediments, heat flow measurements, and for placement of self-contained bottom seismographs, by means of which deep seismic sounding (DSS) was carried out and seismicity was studied.

A great volume of geological and geophysical research was also carried out along the ship's track. It should be noted that for the first time in world practice CSP was carried out at a speed as great as 15 knots; a good quality of the seismic records was maintained. In work by the DSS method use was made of pneumatic sound sources with a great power, this ensuring an adequate depth and detail of investigations of the earth's crust. This made it possible to automate the process of observations and primary processing of records from bottom seismographs.

The extensive geophysical and geological materials collected on the voyage were partially processed aboard the ship. Their laboratory analysis is now continuing. This article gives the most interesting preliminary results obtained by the geomorphology and tectonics, magnetometry and geothermal studies, CSP, DSS and seismology, gravimetry, lithology and stratigraphy, radioisotopic methods and petrography detachments.

The polygon work was begun in the zone of the Atlantis fault. This fault is one of the largest transformed faults in the Atlantic Ocean. It extends in a sublatitudinal direction for almost 2,000 km, approximately between 29° and 30°N. Detailed geological-geophysical investigations of the region of intersection of the fault and crest zone of the Mid-Atlantic Ridge were carried out in 1969 on the sixth voyage of the "Akademik Kurchatov." In this sector the displacement of the axial rift valley of the ridge along the Atlantis fault is about 30 miles; an anomalous structure of the earth's crust was discovered under the fault canyon.

The first geological-geophysical polygon on the 24th voyage of the "Akademik Kurchatov" was situated on the eastern extension of the Atlantis fault at a distance of approximately 700 km from the crest of the Mid-Atlantic Ridge. Here the fault is well expressed in the relief and is represented by two sublatitudinal depressions with depths of 5,500 and 5,800 m. The crests of the rises adjacent to them were situated at depths of 4,000-4,500 m. The steepness of the depression slopes averaged 5-8°, locally attaining 20°.

13

FOR OFFICIAL USE ONLY

FOR OFFICIAL USE ONLY

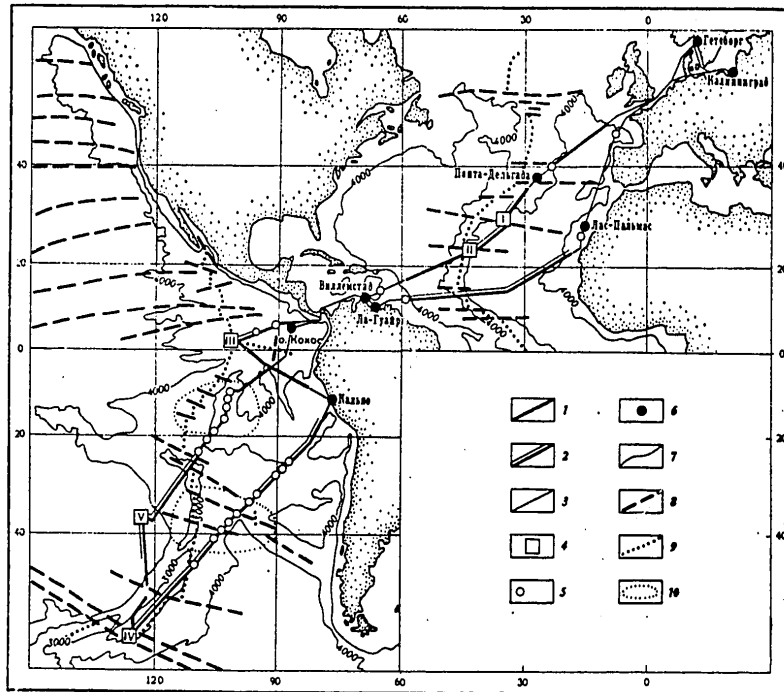


Fig. 1. Track of the 24th voyage of the scientific research ship "Akademik Kurchatov." 1) part of track with depth sounding, magnetometry and gravimetry; 2) part of track with CSP; 3) part of track without magnetometry; 4) polygons; 5) stations; 6) ports of call; 7) isobaths; 8) faults; 9) axes of ridges; 10) regions of metalliferous sediments, I-V) polygons in the fault zones Atlantis, Kane, Galapagos, Eltanin, on western slope of East Pacific Ocean Rise.

In the region of polygon I there was a relatively weak anomalous magnetic field. Here there is a linear positive anomaly, displaced along the fault for approximately 30 miles, as in the rift zone of the mid-oceanic ridge. It is identified as anomaly 24 (age about 60 million years). A positive anomaly corresponds to the central depression of the fault. This depression is characterized by an increased heat flow value.

The depressions of the Atlantis fault correspond to small negative free-air anomalies and positive Bouguer anomalies up to 380 mgal (in the text and in the figures the gravity anomaly values are given in the system of American control points).

FOR OFFICIAL USE ONLY

FOR OFFICIAL USE ONLY

According to CSP data, the sublatitudinal depressions are filled with sediments with a thickness up to 400-800 m. On the slopes of depressions the sedimentary cover is insignificant and in places is absent.

In the depression under the layer of unconsolidated sediments there are rocks in which seismic waves are propagated with a velocity of 5.3 and 7 km/sec. Thus, the deep structure of the Atlantis fault in the investigated sector was as anomalous as in the rift zone of the Mid-Atlantic Ridge.

Rock material in the form of small rock fragments was obtained by three dredges, a heavy corer and a scraper. Hydrothermally modified basalts were raised from the slopes of the southern depression. On the northern slope of the main depression there were basalts, gabbros and serpentinites. It is interesting that in addition to alpinelike hyperbasites and tholeiitic basalts, typical for the rift zones, an alkaline complex of ultrabasites, gabbros and basalts was discovered in the fault.

Thus, the Atlantis fault in the polygon region is a complex echelonlike tectonic zone. The maturity of relief forms, considerable concentrations of sediments, a relatively weak magnetic field, and absence of present-day seismicity is evidence of its antiquity. At the same time, a number of criteria (good expression of the fault in the bottom relief, numerous outcrops of basaltic lavas, increased heat flow values, presence of mudflows, anomalous crustal structure, adaptation of magnetic and gravitational anomalies to the central depression of the fault) indicate its tectonic activity, which, evidently, is intensified periodically as stresses accumulate along the fault.

In polygon II, in the zone of Kane fault, detailed seismic and magnetometric studies were made in the region of borehole 396 by the American ship "Glomar Challenger." The purpose of the work was a comparison of geophysical data on the fine structure of the crust with the results of borehole logging and magnetic measurements in cores. The analysis of the collected materials is still not finished.

The site of polygon II was selected in the neighborhood of Hess depression, situated not far from the crest of the East Pacific Ocean Rise in the zone of the Galapagos fault. Here the preceding expeditions of the Institute of Oceanology discovered sharp bottom relief forms favorable for the dredging of deep crustal rocks. Detailed geomorphological studies in the polygon considerably refined the map of bottom relief in this region. The depth of the Hess depression attains 5,400 m; the northern slope is very steep -- up to 20°. The bottom sectors surrounding the depression are situated at depths of 3-3.5 km.

The magnetic field within the limits of the polygon is characterized by complex positive and negative anomalies with an amplitude up to 750 γ . The maximum negative anomaly is associated with the Hess depression. It is also traced farther -- on the western slope of the East Pacific Ocean Rise, where its intensity gradually decreases. Along both sides of it there is a system of sublatitudinal sign-variable anomalies, complicated by meridional displacements. These anomalies, evidently, are associated

FOR OFFICIAL USE ONLY

with the development of the Galapagos rift zone. All three measurements of the earth's heat flow (two of them were carried out to the west of the Hess depression in the region of the crest of the East Pacific Ocean Rise, and one -- to the south of the depression) gave increased values -- from 2 to 8 heat flow units.

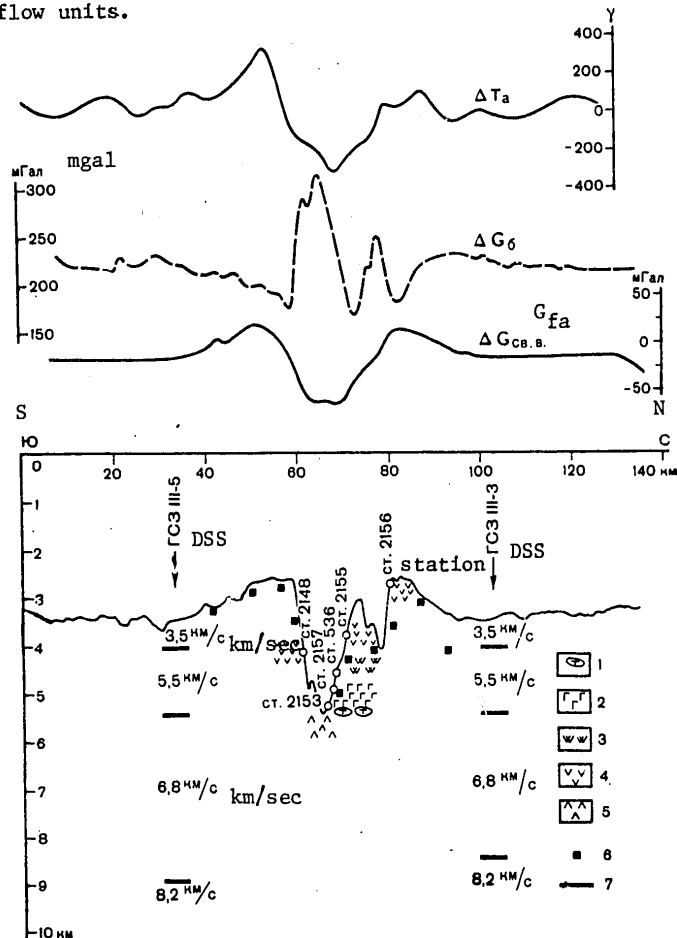


Fig. 2. Geological-geophysical section along meridional profile across Hess depression. 1) lenses and intercalations of plagioclasic olivinites; 2) gabbro complex (troctolites, olivine gabbro-norites, olivine gabbros); 3) dolerites; 4) basalts of the upper complex; 5) basalts of the lower complex; 6) upper surfaces of magnetic bodies; 7) refracting boundaries and velocities according to DSS data, ΔT_a -- curve of magnetic anomalies, ΔG_b -- curve of gravity anomalies in Bouguer reduction, ΔG_{fa} -- curve of free-air gravity anomalies.

FOR OFFICIAL USE ONLY

FOR OFFICIAL USE ONLY

CSP data indicate the absence or very small thickness of unconsolidated sediments both in the depression and in the remaining sectors of the polygon. An analysis of samples of sediments covering small sectors of the Hess depression indicated that they were formed for the most part due to the destruction of bedrock. The deposits bear traces of the effect of thermal springs with which the enrichment of sediments by iron and manganese hydroxyls is associated.

DSS on six profiles situated around the depression yielded quite detailed information on crustal structure. All three investigated sectors are characterized by similar seismic sections, including layers in which the waves are propagated with velocities 3.5, 5.5 and 6.8 km/sec. The Mohorovicic discontinuity is situated at a depth of about 5 km below the bottom surface. In two days bottom seismographs registered about 30 earthquakes, for the most part associated with the Hess depression. Four successive deep dredgings were carried out on the steep northern slope of the depression. The rocks collected on this voyage, and also on the 8th and 14th voyages of the scientific research ship "Dmitriy Mendeleev," make it possible to construct a full section of the oceanic crust (Fig. 2).

The geological section correlates well with respect to the depths and thicknesses of the main layers with a seismic section of the earth's crust: a layer in which waves are propagated with a velocity 3.5 km/sec corresponds to basaltic lavas; a layer in which the velocity of wave propagation is 5.5 km/sec, which corresponds to a basalt-dolerite dike complex; a layer in which the velocity of wave propagation is 6.8 km/sec, corresponding to a complex of gabbroids.

A study of the magnetic properties of the samples indicated that both basalts and gabbro-diabases have a high magnetic susceptibility and remanent magnetization. These two types of rocks evidently also serve as sources of the observed magnetic field anomalies.

The entire complex of investigations carried out in polygon III confirmed the hypothesis of a young rift nature of the Hess depression and made possible a detailed validation of this hypothesis. The rift nature of the depression is indicated by the sharp forms of bottom relief, the absence of a sedimentary cover, hydrothermal phenomena, tholeiitic low-potassium magmatism, high seismic activity, presence of sublatitudinal anomalies and high gradients of the magnetic and gravitational fields. At the same time, it is not precluded that the Hess depression and the entire Galapagos rift zone were formed on a more ancient transformed fault, which, judging from geomorphological, magnetic and gravitational data, continues to the west.

The system of Eltanin faults, on whose northern fault (Heezen fault) polygon IV was selected, is unique with respect to both the scales of horizontal displacements of the ridge crest (about 900 km) and with respect to the sharpness of relief forms — the depth difference along the southern slope of the fault canyon attains 5 km. The idea of studying the Eltanin

FOR OFFICIAL USE ONLY

FOR OFFICIAL USE ONLY

fault on the 24th voyage of the "Akademik Kurchatov" was proposed by Corresponding Members USSR Academy of Sciences A. S. Monin and A. P. Lisitsyn. (A canyon with very steep and high slopes, which attracted the attention of geologists and geophysicists, was discovered in this region during the 14th voyage of the "Dmitriy Mendeleev".)

The system of Eltanin faults was earlier studied using only infrequent reconnaissance profiles. Therefore, the first detailed geological-geophysical studies in polygon IV are interesting in themselves. The investigated sector of the fault is a linear canyon with a northwesterly strike with a depth to 6 km. The steepness of the slopes attains 20-25° (Fig. 3).

In the magnetic field of this region there are linear anomalies parallel to the axis of the East Pacific Ocean Rise, one of which, in the northern block, is tentatively identified as anomaly 4 (age 7 million years). An analysis of the anomalies is evidence of absence of considerable horizontal displacements along Heezen fault. Evidently, the principal displacement occurs along Tarp fault, situated to the south, as is confirmed by seismological data.

The strikes of gravity anomalies coincide with the direction of the fault. Large horizontal field gradients correspond to the canyon slopes. However, the maximum value of the Bouguer anomaly over the fault (+320 mgal) cannot be considered very great, taking into account the depth of the canyon.

According to CSP data, the thickness of the unconsolidated sediments in the polygon is very insignificant, and in many sectors, especially on the steep slopes, there are no sediments.

The results of geological investigations, for the first time carried out in the zone of Eltanin faults, are of exceptional interest. The bedrock material was obtained using four dredges, two scrapers and two concussion corers. On the southern slope, where the depth differential attains 5,100 m, it was possible to obtain a complete section of the earth's crust, including the principal rock complexes (from top to bottom): basaltic, basalt-dolerite, gabbroid and ultrabasic.

The expedition's geologists made two unique finds: on the peak of the southern crest they discovered limestones with Cretaceous coccoliths (determinations by V. V. Mukhina and M. S. Ushakova), and from depths 5,200-5,600 m it was possible to raise enormous blocks of puckered amphibolitic schists. The Cretaceous coccoliths were probably redeposited, since the age of the foraminifera found here is not more ancient than the Upper Miocene (determinations by M. S. Barash). However, the presence of a great amount of Cretaceous and Paleogene coccoliths in the limestones, with an almost complete absence of Neogene-Quaternary coccoliths, can be evidence of the close positioning of shows of Cretaceous and Paleogene rocks, from which material was transported in the Pliocene or in the Miocene. Relatively ancient rocks have already been repeatedly encountered in the axial zone

FOR OFFICIAL USE ONLY

of the mid-oceanic ridge in the Atlantic. This possibly explains the crustal blocks persisting at the center of the ocean which have not been drawn into the spreading process.

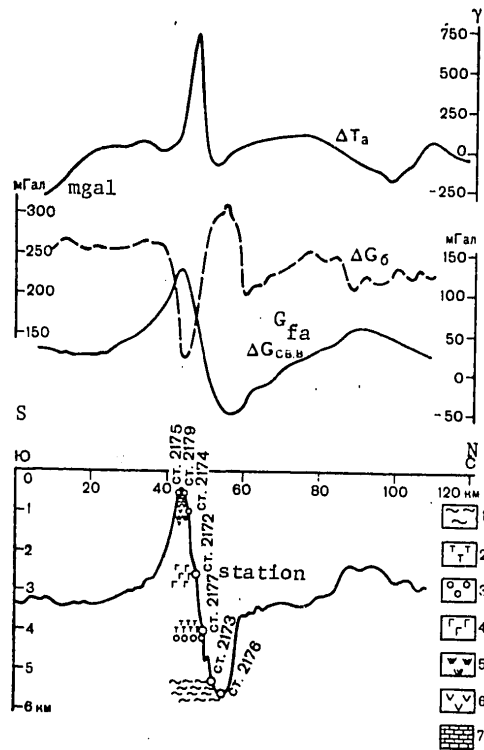


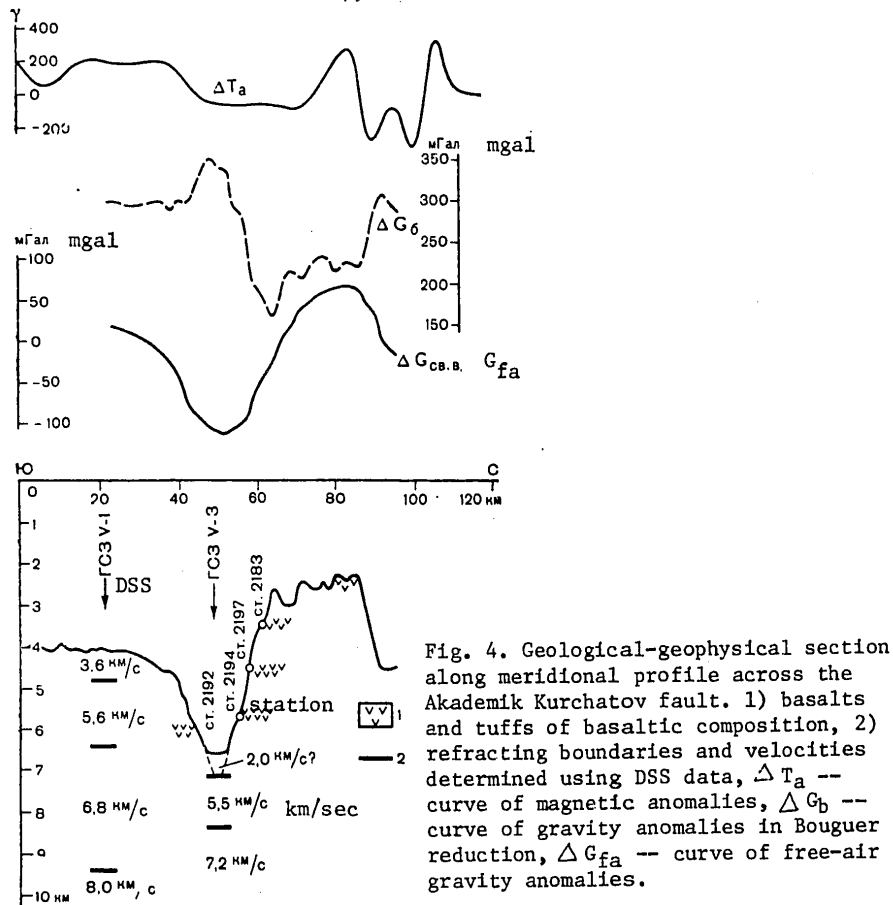
Fig. 3. Geological-geophysical section along meridional profile across the Heezen fault in the system of Eltanin faults. 1) amphibolitic schists; 2) peridotites (Harzburgites, lherzolites); 3) granulites (olivine-, pyroxene-, amphibole-, plagioclase-); 4) gabbro; 5) dolerites; 6) basalts; 7) limestones, ΔT_a -- curve of magnetic anomalies; ΔG_b -- curve of gravity anomalies in Bouguer reduction; ΔG_{fa} -- curve of free-air gravity anomalies.

Amphibolitic schists under such conditions as in polygon IV were found in the ocean for the first time. Two types can be discriminated among them on the basis of mineral composition. One type, the predominant one, is schists enriched with amphibole. Their chemical composition gives basis for assuming that they were formed from tholeiitic basalts, and some from tuffs of this same composition. Schists of another type were found in individual fragments. Their leucocratic composition, with considerable

FOR OFFICIAL USE ONLY

FOR OFFICIAL USE ONLY

quantities of quartz and a small thickness of the intercalations make it possible to postulate that they were formed during the metamorphism of sedimentary rocks of siliceous composition. The degree of metamorphism of the schists corresponds to the facies of epidotic amphibolites. Analyses of amphibolitic schists have not yet been finished. In particular, attempts are being made to determine their absolute age, which in many respects can help in reconstructing tectonic conditions.



FOR OFFICIAL USE ONLY

FOR OFFICIAL USE ONLY

A geophysical survey in polygon V discovered and over an extent of 200 km investigated a new, very large transverse fault intersecting the western slope of the East Pacific Ocean Rise, approximately along 37°S. The maximum depth of the fault canyon was 6,600 m and the depth drop along the highest northern slope in one of the sectors exceeds 5.5 km. Such deep faults were earlier unknown in the East Pacific Ocean Rise. It is proposed that this newly discovered fault be called the "Akademik Kurchatov" fault.

The magnetic field of this investigated region is characterized by considerable anomalies and sharp gradients; the strongest of these are associated with the northern block of the fault (Fig. 4). The fault canyon corresponds to a band of magnetic field negative anomalies.

On the CSP records unconsolidated sediments with a thickness of less than 100 m are noted only in the deepest axial part of the fault; in the remaining regions in the polygon the sedimentary cover is absent or very thin.

DSS revealed an anomalous structure of the earth's crust under a canyon similar in structure to that in the Atlantis fault. The southern block of the crust has a sequence of layers customary for the East Pacific Ocean Rise with a total thickness of about 5 km. In the course of two and a half days of observations the bottom seismographs did not register a single earthquake.

Geological work on the canyon slopes indicated that the fault cuts through a great thickness of basalts and hyaloclastites. The rocks which were raised constitute semirounded, oxidized and weathered fragments with a ferromanganese crust. The presence of tectonic breccias gives basis for postulating that the volcanic stratum is underlain by a metamorphic complex. Phosphatized organogenic limestones are encountered on the northern crest. Geological and geophysical materials indicate a relative antiquity of the Akademik Kurchatov fault.

The investigations carried out during the 24th voyage of the "Kurchatov" confirmed the great possibilities of detailed geological-geophysical studies in zones of transformed faults for study of deep layers of the earth's crust which for the time being are inaccessible for oceanic drilling. For example, in the Hess depression and in the Heezen fault it was possible to obtain complete sections of the earth's crust. A comparison of these sections with seismic and geomagnetic data made it possible to refine the nature of the seismic layers and detect the principal sources of magnetic field anomalies.

It has been established that transformed faults, even at a considerable distance from the rift zones of the mid-oceanic ridges, retain the anomalous structure of the earth's crust, specific magmatism and anomalies of geophysical fields associated with them. As indicated by geological and geophysical data, the studied faults evidently are inherited structures

FOR OFFICIAL USE ONLY

which penetrate to a great depth. Their tectonic activity does not cease beyond the limits of the rift zones.

Lithological studies along two sections -- across the eastern slope of the East Pacific Ocean Rise and in the Bauer depression -- made it possible to refine the boundaries of regions of propagation of metalliferous sediments and study the facies types of these sediments. Investigations of the field of metalliferous sediments indicated that manifestations of the presence of metals both along the axial zone of the rise and in the zones of transformed faults vary and anomalously high contents of iron, manganese and other accompanying elements have a strictly local character. A new region of high metal content of deposits was discovered in the zone of contact between the East Pacific Ocean and West Chilean Rises. The Pleistocene noncalcareous pelagic oozes here contain up to 25% iron and up to 7% manganese. The materials from this and preceding expeditions (8th and 14th voyages of the scientific research ship "Dmitriy Mendeleev") indicate that genetically the metalliferous sediments are associated with hydrothermal activity and its activity plays a decisive role in the formation of these deposits. In turn, hydrothermal springs are associated with active faults in the earth's crust.

As indicated by the expedition results, detailed geological and geophysical investigations of zones of deep faults on the ocean floor give very valuable materials necessary for understanding the processes involved in the formation of the earth's crust, refinement of the nature of the principal crustal layers and anomalies of geophysical fields, determination of the scales of ore shows and their prospects. Therefore, further systematic multisided study of these zones is of great importance.

COPYRIGHT: Izdatel'stvo "Nauka," "Vestnik Akademii nauk SSSR," 1979

[496-5303]

FOR OFFICIAL USE ONLY

UDC 550.373

GEOMAGNETIC FIELD DISTURBANCES CREATED BY SEA CURRENTS

Moscow GEOMAGNETIZM I AERONOMIYA in Russian Vol 19, No 4, 1979 pp 708-714

[Article by S. S. Perepelkin, B. I. Verkin, I. O. Kulik and R. I. Shekhter, Physical-Technical Institute of Low Temperatures Ukrainian Academy of Sciences, submitted for publication 19 April 1978]

Abstract: The authors computed the spatial distribution of the magnetic field generated by the movement of a jet of conducting fluid in a layer of finite thickness in a constant external field H^0 . The article gives numerical estimates of the geomagnetic disturbances created by sea currents of different scales.

[Text] At the present time, in connection with active interest in study of the world ocean, attention is being given to the possibility of studying sea currents and other sea movements [1] on the basis of the secondary magnetic fields created by them. Reference is to fields generated by the movement of a conducting fluid in the earth's permanent magnetic field. In this study the problem has been solved for jet movements of the sea, taking into account both the longitudinal and rotational components of velocity in the jet. An important consideration is allowance for influence of the sea water - air discontinuity, deforming the streamlines and screening the magnetic field over the conducting medium. As a result, the magnetic field in the air is extremely small, although in principle it can be registered by modern magnetometers [2, 3]. Since the magnetic fields created by a disturbance of the surface layers of the sea decrease exponentially with depth [4-7], measurements within the sea, at an adequate distance from its surface, can become an effective method for studying deep currents.

Distribution of magnetic field in a fluid with an arbitrary velocity field. A determination of fields in a moving conducting medium involves the joint solution of the Maxwell equations and the Navier-Stokes equations, determining the dynamics of the fluid [8, 9]. A precise solution of the problem requires stipulation of the sources generating the currents, but this goes beyond the framework of this article.

FOR OFFICIAL USE ONLY

FOR OFFICIAL USE ONLY

Due to the weakness of the earth's field it is possible to neglect its influence on the nature of the current and take into account only the magnetohydrodynamic effects in the permanent magnetic field H^0 . Therefore, being interested in the problem of detection of magnetic fields associated with currents, it is possible to formulate the problem of electromagnetic disturbances induced by a stipulated hydrodynamic velocity field $v(r)$, leaving to one side the problem of the formation of currents. In a stationary case, when there is sufficiently slow movement $|v| \ll c$, determining the electric E and magnetic H fields, has the form [10-11]:

$$\begin{aligned} \text{rot } H &= (4\pi/c)j, \quad \text{div } H = 0, \quad \text{rot } E = 0, \quad \text{div } j = 0, \\ j &= \sigma \{E + c^{-1}[v \times H^0]\}, \end{aligned} \quad (1)$$

where j is the density of the induced current, σ is conductivity of the medium.

In the case of small values of the Reynolds magnetic number R_m the system of equations (1) can be solved with the arbitrary dependence $v(r)$. The solution has the form

$$H = H^0 + \frac{1}{4\pi\gamma_m} \int \frac{(cE + v \times H^0) \times R}{R^3} dV, \quad E = \frac{1}{4\pi c} \int \frac{\nabla(H^0 \text{ rot } v)}{R} dV, \quad (2)$$

where $\gamma_m = c^2/4\pi\sigma$ is the magnetic viscosity of the medium, R is the radius vector drawn from an element of the volume dV to the observation point. [$R_m = va/\gamma_m$, where v is the characteristic velocity value, a is the linear dimension.]

The solution (2) is correct in an unbounded medium. In the presence of surfaces or discontinuities of the media, other than the ordinary conditions of regularity imposed on the functions $E(r)$, $H(r)$, it is necessary to require satisfaction of the corresponding boundary conditions. In particular, on the boundary with the nonconducting medium it is necessary to require satisfaction of the conditions of nonpassage of an electric current through the discontinuity:

$$(\overline{E} + c^{-1}v \times H^0)n = 0, \quad (3)$$

where n is the normal to the surface. The corresponding solution can be obtained from (2) by the images method (for a plane discontinuity) and is analyzed below for specific examples of currents.

Field of linear rotating jet. We will stipulate the distribution of velocities in a fluid in the form (in a cylindrical coordinate system) $v_r = 0$, $v_\varphi = u(r)\theta(a-r)$, $v_z = 0$, where $\theta(x)$ is a Heaviside step function, that is, we will assume that the fluid rotates in a tube with the radius a with a distribution of the velocity of rotation along the radius $u = u(r)$.

FOR OFFICIAL USE ONLY

FOR OFFICIAL USE ONLY

The sea water - air discontinuity, parallel to the axis of the jet, passes at the distance d from the axial line of the jet. The outer magnetic field H^0 is oriented arbitrarily relative to the jet. Using expressions (1), (2) we find the components of the H fields and current density:

$$h_r = (H_{\perp}^0/2v_m) \{ [u_0(r) - u_0(a) - r^{-2}u_2(r)]\theta(a-r) - r^{-2}u_2(r)\theta(r-a) \} \cos \varphi, \quad (4a)$$

$$h_{\varphi} = (H_{\perp}^0/2v_m) \{ [u_0(a) - u_0(r) - r^{-2}u_2(r)]\theta(a-r) - r^{-2}u_2(r)\theta(r-a) \} \sin \varphi, \quad (4b)$$

$$u_n(r) = \int_0^r u(\rho) \rho^n d\rho, \quad (5)$$

$$E_r = -(H_z^0/c)u(r)\theta(a-r), \quad j_z = -(\sigma u(r)H_{\perp}^0/c)\theta(a-r) \sin \varphi$$

(the omitted components are equal to zero). H_{\perp}^0 , H_z^0 are the magnetic field components directed perpendicular to the axis of the jet and along it, $h = H - H^0$ are disturbed fields related to rotation.

As can be seen from the formulas (4a, 4b), the magnetic field decreases with distance in conformity to the law $h \sim r^{-2}$, which corresponds to the field of an infinitely long magnetized filament with a magnetic moment of a unit length dependent on the radius of the jet and the second moment of the velocity of rotation $u_2(a)$: $m = H_{\perp}^0 u_2(a) / 4 v_m$.

We note that the electric current arising in the medium is determined only by the magnetic field component transverse to the axis of the jet and localized within it. It follows from expression (5) that the total current in the jet section is equal to zero. Therefore, the determined distribution of the induced fields is not dependent on the presence of a discontinuity and is correct both within the fluid and outside it. The order of magnitude of magnetic field strength in the air is determined by the expression

$$h \sim h_0 a^2 / 3r^2,$$

where h_0 is expressed through the value of the Reynolds number

$$h_0 = H_{\perp}^0 R_m / 2. \quad (6)$$

Magnetic field of a linear jet with a longitudinal velocity component. The role of the sea water - air discontinuity is more significant in the presence of longitudinal movement of the fluid in the jet. For the purpose of studying this problem we will stipulate the velocity distribution in the form $v_r = 0$, $v_{\varphi} = 0$, $v_z = v \theta(a - r)$ and again we will use expression (2). We obtain for the case of an unbounded medium

$$\begin{aligned} E_r &= -(H_{\perp}^0 v / 2c) \chi(a/r) \operatorname{sign}(r-a) \cos \varphi, & E_{\varphi} &= -(H_{\perp}^0 v / 2c) \chi(a/r) \sin \varphi, \\ h_z &= -(H_{\perp}^0 R_m / 2) [(r/a) \theta(a-r) + (a/r) \theta(r-a)] \sin \varphi, & & (7) \\ j_r &= -(\sigma v H_{\perp}^0 / 2c) \chi(a/r) \cos \varphi, \\ j_{\varphi} &= -(\sigma v H_{\perp}^0 / 2c) \chi(a/r) \operatorname{sign}(r-a) \sin \varphi. \end{aligned}$$

FOR OFFICIAL USE ONLY

FOR OFFICIAL USE ONLY

Here we have introduced the function $\chi(x) = \theta(1-x) + x^2\theta(x-1)$. [We note that the cited expression for the magnetic field h_z at great distances $r \gg a$ coincides with the results in [12] for a jet with exponentially blurred edges.]

As can be seen from formulas (7), the electric field and the current are determined by the component of the permanent field $H_{\perp 0}$ and in contrast to the case of rotational movement are propagated through the entire conducting medium, relatively slowly dropping off with increasing distance from the axis of the jet $j \sim r^{-2}$. However, the distributions (7) are not applicable near the discontinuity, where the current pattern is substantially deformed.

The solution satisfying the boundary condition (3) is reduced to a suitable choice of systems for representations of jets situated equidistantly outside the conducting layer. The center of the jet is situated at the distance $\lambda/2 - d$ from the "core" of the plane conducting layer, the layer thickness λ (see inset in Fig. 1). The distribution of the magnetic field has the form of an infinite sum for all images. Transforming the corresponding expressions by means of the Poisson summation formula [13], it is possible to represent the final distribution of the additional field in the following form:

$$h_r = h_\varphi = 0, \quad h_z = h_z^0 \theta(a-r) - (\pi R_m a / 4l) (H_z^0 \psi_x + H_y^0 \psi_y),$$

$$h_z^0 = -(R_m / 2) [H_z^0 (r/a - a/r) \cos \varphi + H_y^0 (r/a - a/r) \sin \varphi], \quad (8)$$

where

$$\psi_x = \frac{\text{sh } \pi x / l}{\text{ch } \pi x / l - \cos \pi y / l} - \frac{\text{sh } \pi x / l}{\text{ch } \pi x / l - \cos \pi (y-2d) / l}, \quad (9)$$

$$\psi_y = \frac{\sin \pi (y-2d) / l}{\text{ch } \pi x / l - \cos \pi (y-2d) / l} + \frac{\sin \pi y / l}{\text{ch } \pi x / l - \cos \pi y / l}.$$

We note that the currents generated by a linear jet lie in a plane perpendicular to its axis and limited by the thickness of the conducting layer. The distribution of the magnetic field within the layer over the jet ($x = 0$) for different positionings of the jet is shown in Fig. 1. The solid curve corresponds to a jet situated in the middle ($d = \lambda/2$), the dashed curve represents the current depth $d = 3\lambda/4$. The y' coordinate is reckoned from the middle of the layer. The field scale is determined by the parameter h_0 , determined by formula (6), in which as v it is necessary to take the velocity of longitudinal movement.

According to the results, the field at the boundary of the layer (the same as the current component normal to the boundary) becomes equal to zero. From the continuity condition and the Maxwell equations it should also become equal to zero at any point outside the conducting medium. The determined field distribution resembles the result correct in the case of two infinitely long solenoids. Thus, the role of the discontinuity is reduced to the screening of the field of an infinite jet outside the conducting medium.

FOR OFFICIAL USE ONLY

FOR OFFICIAL USE ONLY

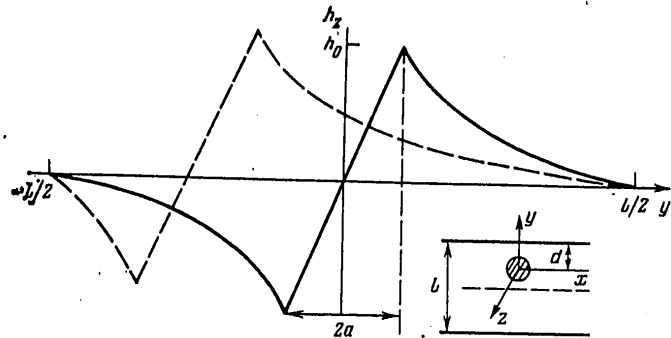


Fig. 1.

To be sure, a real jet has a limited length. Assuming this length to be equal to $2L$ and stipulating the velocity distribution

$$v_z = v\theta(a-r)\theta(L-|z|), \quad (10)$$

we will evaluate the arising "scattering fields" outside the fluid.

The velocity distribution (10) is characteristic of a current created by the inflow and outflow operative at the points $z = \pm L$. In actuality, a jet of a finite length must have a transition region where ordered translational movement, scattering, disappears. The model which we adopted takes into account the contribution to the magnetic field from currents generated by the translational movement of the fluid in the jet and the contribution of the random currents arising as a result of the complex, unordered movement of the fluid near the ends of the jet is neglected.

Substituting the distribution of the electric current in the Biot-Savart formula in the form $j = j_0 \theta(L - |z|)$, where j_0 is determined from solution of the boundary problem similar to (8), (9), we obtain the distribution of the additional field in outer space. We will not fully write the corresponding distribution due to unwieldiness and we will cite only the asymptotic form at great distances $|R| \gg 1$:

$$h_x = -\frac{R_m H_0^0 a}{4l} \left(\frac{d}{l} - \frac{1}{2} \right) F_1, \quad h_y = h_x \frac{Y}{X}, \quad h_z = \frac{R_m H_0^0 a}{4l} \left(\frac{d}{l} - \frac{1}{2} \right) F_2, \quad (11)$$

$$F_1 = \frac{X}{(R^2 + Z_1^2)^{3/2}} - \frac{X}{(R^2 + Z_2^2)^{3/2}}, \quad (12)$$

$$F_2 = \frac{Z_1}{(R^2 + Z_1^2)^{3/2}} + \frac{Z_2}{(R^2 + Z_2^2)^{3/2}},$$

FOR OFFICIAL USE ONLY

FOR OFFICIAL USE ONLY

where $X = x/l$, $Y = y/l$, $Z = z/l$ are the reduced coordinates of the observation point; $Z_{1,2} = L/l \mp Z$; R is the distance from the center of the jet to the observation point in the cited coordinates.

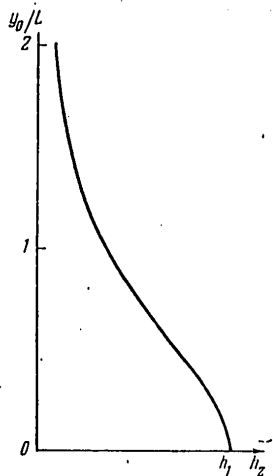


Fig. 2.

As can be seen from expressions (11), the direction of the additional field is dependent on the positioning of the jet relative to half sea depth. In a case when the depth of the jet is equal to half the thickness of the fluid layer, the magnetic disturbance in a dipole approximation (11) becomes equal to zero. The field distribution (11) is illustrated in Fig. 2, which shows the horizontal field component directly over the jet ($x = 0$, $z = 0$) as a function of y_0 -- the distance to the sea surface. The field scale in the air is determined by the expression

$$h_1 \sim h_0 a l L^{-2} (d/l - 1/2),$$

which tends to zero when $L \rightarrow \infty$.

Numerical estimates of geomagnetic disturbances. The results make it possible to estimate the geomagnetic disturbances of the jet. Their value and the law of decrease with distance are determined both by the parameters of the jet and by the distance to the observation point in the sea or in the air. At the same time that the disturbance of the rotating jet conforms to a law correct for the magnetized filament, the nature of the asymptotic form of the magnetic field in a translationally moving jet changes considerably with movement along its length. It is interesting to compare the characteristic magnitudes of the geomagnetic disturbances created by the translational and rotational movements of the fluid.

FOR OFFICIAL USE ONLY

FOR OFFICIAL USE ONLY

Table 1 gives the characteristic values of the geomagnetic disturbances of a jet for different current conditions and observation regions (a is the radius of the jet, 2L is its length, ℓ is sea depth), R_m^{rot} and R_m^{trans} are the values of the Reynolds magnetic number for the rotational and translational components of jet velocity. In a case when translational and rotational components of jet movement exist simultaneously, their contribution is summed. The values cited in Table 1 determine the maximum field values, their dependence on distance is determined by the more detailed expressions derived above.

When $R \ll L$, that is, at a distance from the jet small in comparison with its length, the fields in the air for translational and rotational movements are related as

$$h^{trans}/h^{rot} \sim v_0 l R^2 / u_0 a L^2,$$

where v_0 is the characteristic velocity of the translational and u_0 is the characteristic velocity of rotational movements. The magnetic field of a rotating jet decreases in the outer space in conformity to the law R^{-2} , slower than the field of the magnetic dipole $h \sim R^{-3}$. For a jet of finite length or a jet having a curvature of its movement at the characteristic distance L, this law will be correct at distances from it not exceeding L. Such currents can be registered relatively easily. A similar conclusion can evidently be drawn for local disturbances of the jet associated with rotation. When $R \gg L$ the magnetic field of a limited longitudinal jet decreases with distance in conformity to the law R^{-3} and at short distances attains saturation (see Fig. 2).

Table 1

Характер движения	1	Внутри моря	2	3 В воздухе
4	Вращающаяся струя	$H_{\perp}^0 R_m^{rot} / 6$	6	$H_{\perp}^0 R_m^{rot} / 6$
5	Струя с продольным движением	$H_{\perp}^0 R_m^{post} / 2$	7	$H_{\perp}^0 R_m^{post} a l / 2 L^2$

KEY:

- | | |
|-----------------------------------|------------------|
| 1. Nature of movement | 6. rotational |
| 2. Within sea | 7. translational |
| 3. In air | |
| 4. Rotating jet | |
| 5. Jet with longitudinal movement | |

Table 2

L, км	У ₀ , км					L, км	У ₀ , км				
	-0,5	0	5	10	100		-0,5	0	5	10	100
5	1	0,05	0,01	0,004	$6 \cdot 10^{-6}$	100	1	10^{-4}	10^{-4}	10^{-4}	$4 \cdot 10^{-5}$
10	1	0,01	0,008	0,005	10^{-5}	1000	1	10^{-6}	10^{-6}	10^{-6}	10^{-6}

FOR OFFICIAL USE ONLY

FOR OFFICIAL USE ONLY

Table 3

a, M	y ₀ , KM				a, M	y ₀ , KM			
	1	5	10	100		1	5	10	100
50	0,001	2·10 ⁻⁴	4·10 ⁻⁵	10 ⁻⁶	250	0,2	0,01	0,005	6·10 ⁻⁵
100	0,01	0,001	3·10 ⁻⁴	5·10 ⁻⁶	1000	10	1	0,3	4·10 ⁻³

Tables 2, 3 give numerical estimates of geomagnetic disturbances obtained for a number of values of the L and R parameters of practical interest corresponding to both large-scale ocean currents and to relatively small jet disturbances [14]. Table 2 gives the values of the geomagnetic disturbances (in gammas) created by the translational movement of a fluid in a jet when $a = 100$ m, $d = 1$ km, $\lambda = 4$ km, $\sigma = 4$ Cm/m, $v = 10^2$ cm/sec; $y_0 = -0.5$ corresponds to the field of an infinitely long jet within a fluid layer at the depth 500 m, $y_0 = 0$ is the sea surface. Table 3 gives the values of the geomagnetic disturbances (in gammas) for a rotational movement of the fluid in the jet when $d = 1$ km, $\sigma = 4$ Cm/m, $u = 10^2$ cm/sec. As can be seen from the cited data, the field disturbances can vary in a wide range from fractions of a gamma to 10^{-6} gamma. The existence at the present time of superconducting magnetometers [15] makes it possible to register magnetic fields to 10^{-6} γ and their gradients $\sim 10^{-6}$ γ/cm . In a study of deep currents it can be of interest to measure the field within the sea at a relatively short distance from the surface (such, however, that it is possible to neglect the exponentially decreasing field of sea waves). According to Table 2, in this case the field strength of the jet is considerably greater than the field outside the fluid.

We note in conclusion that the computations made relate formally not only to disturbances created by sea movements, but also circumterrestrial plasma. Therefore, observations from aircraft and artificial earth satellites with superconducting apparatus on board can be a convenient tool for studying the spatial and temporal variations of the geomagnetic field of both hydro-spheric and ionospheric origin.

The authors express appreciation to Professor B. Ya. Levin for discussion of the results.

BIBLIOGRAPHY

1. Shuleykin, V. V., FIZIKA MORYA (Marine Physics), "Nauka," 1968.
2. Solimar, L., TUNNEL'NYE EFEKTY V SVERKHPROVODNIKAKH I YEGO PRIMENENIYE (The Tunnel Effect in Superconductors and its Use), "Mir," 1974.
3. Kulik, I. O., Yanson, I. K., EFEKTY DZHOZEFSONA V SVERKHPROVODYASHCHIKH TUNNEL'NYKH STRUKTURAKH (Josephson Effect in Superconducting Tunnel Structures), "Nauka," 1970.

FOR OFFICIAL USE ONLY

FOR OFFICIAL USE ONLY

4. Weaver, J. T., JGR, 70, 1921, 1965.
5. Leybo, A. B., Semenov, V. Yu., GEOMAGNETIZM I AERONOMIYA (Geomagnetism and Aeronomy), 15, 231, 1975.
6. Podney, W., JGR, 80, 2977, 1975.
7. Gorskaya, Ye. N., Skrynnikov, R. G., Sokolov, G. V., GEOMAGNETIZM I AERONOMIYA, 12, 153, 1972.
8. Kontorovich, V. M., DOKL. AN SSSR (Reports of the USSR Academy of Sciences), 137, 576, 1961.
9. Burtsev, G. A., IZV. AN SSSR, FIZIKA ATMOSFERY I OKEANA (News of the USSR Academy of Sciences, Physics of the Atmosphere and Ocean), 11, 1084, 1975.
10. Tikhonov, A. N., Sveshnikov, A. G., IZV. AN SSSR, SER. GEOFIZ. (News of USSR Academy of Sciences, Geophysical Series), No 1, 48, 1959.
11. Landau, L. D., Lifshits, Ye. M., ELEKTRODINAMIKA SPLOSHNYKH SRED (Electrodynamics of Continuous Media), Moscow, 1959.
12. Dorman, L. I., VOPROSY MAGNITNOY GIDRODINAMIKI I DINAMIKI PLAZMY (Problems in Magnetohydrodynamics and Dynamics of Plasma), AN LatvSSR, 63, 1962.
13. Korn, G., Korn, T., SPRAVOCHNIK PO MATEMATIKE (Mathematics Handbook), "Nauka," 1974.
14. Kamenkovich, V. M., OSNOVY DINAMIKI OKEANA (Principles of Ocean Dynamics), "Nauka," 1973.
15. Goodman, W. L., Hesterman, V. W., Rorden, H., Goree, W. S., PROC. IEEE, 61, 20, 1973.

COPYRIGHT: Izdatel'stvo "Nauka," "Geomagnetizm i aeronomiya," 1979

[495-5303]

FOR OFFICIAL USE ONLY

FOR OFFICIAL USE ONLY

UDC 550.373

ELECTROMAGNETIC FIELD OF SEA WAVES IN AN ELECTRICALLY STRATIFIED SEA

Moscow GEOMAGNETIZM I AERONOMIYA in Russian Vol 19, No 4, 1979 pp 715-721

[Article by V. P. Smagin and V. N. Savchenko, Far Eastern State University, submitted for publication 30 May 1978]

Abstract: The authors formulate and solve the problem of an induced electromagnetic field of sea wind waves in an electrically stratified sea of finite depth. Sea conductivity is stipulated as a function exponentially decreasing with depth. Electric field strength and the field of magnetic induction are found from solutions of the equations for scalar potential.

[Text] Introduction. The problem of the influence of electric stratification of extended conductors of finite thickness on the form of the variable electromagnetic field inside and outside these conductors is of great importance for geophysics [1, 2]. As noted in [3], the electric stratification of the earth is important for study of both electric currents in the ocean and the conductivity of bottom rocks. But in that study there was no discussion of the role of electric stratification of the ocean itself. However, experimental data on conductivity of the ocean throughout its thickness indicate its sharp change, especially in the surface layer with a thickness of 1 km [4]. This circumstance encourages development of a variant of the theory of electromagnetic induction in the ocean which would take into account the nonuniformity of conductivity in the ocean, the diversity of types of wave movement of the sea medium (potential or eddy) and an arbitrary choice of an electric model of the bottom. This problem has not been solved in the studies known to us (see reviews [3-5]).

Equations for electric and magnetic fields and electric potential in an electrically stratified ocean. For solving problems related to electromagnetic induction in the ocean we will select a system of Maxwell equations in a quasistationary approximation, which is adequately substantiated [6, 7] for the range of characteristic frequencies of sea waves, taking into account

FOR OFFICIAL USE ONLY

FOR OFFICIAL USE ONLY

the low conductivity of the sea medium. However, for deriving the equations of magnetic induction and an electric field, taking into account the nonuniformity of conductivity $\sigma(r)$ of the sea medium, in the initial system of equations for the electromagnetic field we retain the displacement currents which we will neglect after completing derivation of the mentioned equations.

We will use the following Maxwell equations (in a practical system of units):

$$\text{rot } \mathbf{B} = \mu(\mathbf{j} + \partial \mathbf{D} / \partial t), \text{ rot } \mathbf{E} = -\partial \mathbf{B} / \partial t, \text{ div } \mathbf{D} = \rho, \text{ div } \mathbf{B} = 0, \quad (1)$$

supplemented by the system of relationships

$$\mathbf{D} = \epsilon \mathbf{E}, \mathbf{B} = \mu \mathbf{H}, \mathbf{j} = \sigma(\mathbf{E} + [\mathbf{v} \times \mathbf{B}]). \quad (2)$$

Henceforth the sea medium is assumed to be nonmagnetic, that is, $\mu = \mu_0$, where μ_0 is the magnetic permeability of a vacuum. In Ohm's law (2) \mathbf{v} is the velocity of movement of the fluid, to be more precise, the velocity of movement of its particles. The \mathbf{B} field includes the permanent geomagnetic field and the induced magnetic field, which is considerably less than the geomagnetic field, as a result of which in $[\mathbf{v} \times \mathbf{B}]$ (2) we will retain only the term $[\mathbf{v} \times \mathbf{F}]$.

We will also assume that sea waves of all types contain an oscillating temporal factor $\exp(-i\omega t)$ which also contains electromagnetic values. We will make partial use of this circumstance in the derivation of equations for \mathbf{B} and \mathbf{E} .

For \mathbf{B} we obtain an equation in a quasistationary approximation

$$\Delta \mathbf{B} + \text{grad } \ln \sigma \times \text{rot } \mathbf{B} - \mu \sigma \partial \mathbf{B} / \partial t = -\mu \sigma (\mathbf{F} \cdot \nabla) \mathbf{v}, \quad (3)$$

for \mathbf{E} , on the other hand:

$$\Delta \mathbf{E} + \text{grad}(\mathbf{E} \cdot \text{grad } \ln \sigma) - \mu \sigma \frac{\partial \mathbf{E}}{\partial t} = -\text{grad}\{\mathbf{F} \text{ rot } \mathbf{v} + [\mathbf{v} \times \mathbf{F}] \text{grad } \ln \sigma\}. \quad (4)$$

Equations (3) and (4) must be supplemented by boundary and boundary-value conditions, without which it is impossible to attain unambiguity of the solution. First we will assume the disappearance of all fields at infinity.

The boundary conditions for the fields of conductors formed from sectors of different conductivity are well known within the framework of a quasistationary approximation [8]. Due to the nonmagnetic nature of the sea medium there is a continuity of the magnetic induction vector \mathbf{B} on all the conductivity discontinuities. The continuity of the tangential component B_τ leads to a continuity of the normal component $(\text{rot } \mathbf{B})_n$ or a continuity $\mu \sigma (\mathbf{E} + [\mathbf{v} \times \mathbf{F}])_n$. The continuity of the normal component B_n leads, in accordance with (1), to continuity of the normal component $(\text{rot } \mathbf{E})_n$ or a continuity of the tangential component E_τ .

FOR OFFICIAL USE ONLY

Without analyzing equations (3) and (4) and without seeking methods for their solution, we will go in the direction of a further simplification of the conditions of the problem, assuming that it is possible to neglect the effect of self-induction in equations (1), as has been done in other studies [9-11]. The latter assumption leads to a restriction on the range of the frequency spectrum of sea waves (and the electromagnetic field) by the inequality $k^2 \gg \mu \sigma \omega$, which is easy to obtain from a comparison of the Laplace operators Δ and $-\mu \sigma \partial / \partial t$ after their effect on a plane monochromatic wave (in hydrodynamics -- a surface progressive wave), propagating in the direction of the x-axis.

With the assumptions made the system of equations has the form:

$$\begin{aligned} \operatorname{rot} \mathbf{B} = \mu \mathbf{j}, \operatorname{rot} \mathbf{E} = 0, \operatorname{div} \mathbf{j} = 0, \\ \operatorname{div} \mathbf{B} = 0, \operatorname{div} \mathbf{D} = \rho, \mathbf{j} = \sigma (\mathbf{E} + [\mathbf{v} \times \mathbf{F}]), \end{aligned} \quad (5)$$

hence the electric field \mathbf{E} can be stipulated through the potential: $\mathbf{E} = -\operatorname{grad} \varphi$.

Introducing $\sigma = \sigma(z)$ and limiting ourselves only to the vertical component of the geomagnetic field $\mathbf{F} = k\mathbf{F}$, from the equation $\operatorname{div} \mathbf{j} = 0$ we obtain:

$$\operatorname{div} \mathbf{E} = -\mathbf{F} \operatorname{rot} \mathbf{v} - \mathbf{E} \operatorname{grad} \ln \sigma,$$

and then for electric potential -- the equation:

$$\Delta \varphi + \operatorname{grad} \ln \sigma \operatorname{grad} \varphi = \mathbf{F} \cdot \operatorname{rot} \mathbf{v}. \quad (6)$$

In deriving the equations it was taken into account that $[\mathbf{v} \times \mathbf{F}] \operatorname{grad} \ln \sigma \equiv 0$.

Now it is necessary to determine the nature of the wave movement of the sea medium. The ocean will be assumed to have the constant depth H and to be unbounded in the horizontal plane.

The system of Cartesian coordinates is situated on the undisturbed sea surface; the z-axis is directed vertically upward, the x and y axes lie in the horizontal plane. A sea wave, which is selected in the form proposed in [10], has a component of the velocity of motion of fluid particles in the horizontal plane along the x axis and assumes a periodic change in the velocity of motion of fluid particles in the direction of the y axis. The finite length of the wave crest is thereby taken into account. The horizontal velocity of the fluid particles along the x axis is stipulated in the form:

$$v = v(z, k) \cos(nx - \omega t) \cos my, \quad (7)$$

where $n = 2\pi / \lambda_x$; $m = 2\pi / \lambda_y$; $\omega = 2\pi / T$, λ_x , λ_y are the wave lengths in the directions of the x and y axes respectively; T is the period of oscillations; $k^2 = n^2 + m^2$. We will substitute the expression for velocity (7) into (6), after which the right-hand side of the potential equation becomes

FOR OFFICIAL USE ONLY

equal to $mFv(z, k) \cos (nx - \omega t) \sin my$. It is natural to seek solutions of the equation by the separated variables method

$$\varphi(x, y, z) = \varphi(z, k) \cos (nx - \omega t) \sin my.$$

As a result, the equation for potential amplitudes is written in the form

$$\frac{\partial^2 \varphi(z, k)}{\partial z^2} + \frac{d}{dz} \ln \sigma(z) \frac{\partial \varphi(z, k)}{\partial z} - k^2 \varphi(z, k) = mFv(z, k). \quad (8)$$

Equation (8) is fundamental for further investigations. Assuming different models of waves and conductivity, that is, stipulating the functions $v(z, k)$ and $\sigma(z)$, using (8) it is possible to determine the electric potential, and already on the basis of the potential -- the electric currents and magnetic fields in all media.

Equation (8) is supplemented by the continuity conditions for the normal component of electric current density and the already noted continuity E_z at the conductivity discontinuities.

Assume that solutions of equation (8) have been found (a specific example of the solution will be given in the next section). We will show that the remaining electromagnetic parameters can be determined in the latter.

The electric field components are expressed most simply:

$$\begin{aligned} E_x &= -\partial \varphi(x, y, z) / \partial x = n \varphi(z, k) \sin (nx - \omega t) \sin my, \\ E_y &= -\partial \varphi(x, y, z) / \partial y = -m \varphi(z, k) \cos (nx - \omega t) \cos my, \\ E_z &= -\partial \varphi(x, y, z) / \partial z = -[d \varphi(z, k) / dz] \cos (nx - \omega t) \sin my. \end{aligned} \quad (9)$$

Using Ohm's law, we will determine the components of the current density vector j :

$$\begin{aligned} j_x &= \sigma E_x = n \sigma(z) \varphi(z, k) \sin (nx - \omega t) \sin my = \\ &= j_x(z) \sin (nx - \omega t) \sin my, \\ j_y &= \sigma(E_y - vF) = -\sigma(z) [m \varphi(z, k) + Fv(z, k)] \cos (nx - \\ &\quad - \omega t) \cos my = j_y(z) \cos (nx - \omega t) \cos my, \\ j_z &= \sigma E_z = -\sigma(z) [d \varphi(z, k) / dz] \cos (nx - \omega t) \sin my = \\ &= j_z(z) \cos (nx - \omega t) \sin my. \end{aligned} \quad (10)$$

The induced current creates magnetic induction $B(r)$, which we will determine using the Biot-Savart law

$$\mathbf{B}(r) = \frac{\mu_0}{4\pi} \iiint \frac{[\mathbf{j}(r') \times (\mathbf{r} - \mathbf{r}')]}{|\mathbf{r} - \mathbf{r}'|^3} d\mathbf{r}'.$$

Here r is the radius-vector of the observation point; r' are the radius-vectors of the points of electric current sources. Integration is carried out for the entire region of electric currents.

First we will find the vertical component of magnetic induction:

$$B_z(x, y, z) = \frac{\mu_0}{4\pi} \iiint \frac{j_x(x', y', z')(y - y') - j_y(x', y', z')(x - x') dx' dy' dz'}{[(x - x')^2 + (y - y')^2 + (z - z')^2]^{3/2}}. \quad (11)$$

FOR OFFICIAL USE ONLY

FOR OFFICIAL USE ONLY

We introduce the notations $\xi = x' - x$, $\eta = y' - y$, $\zeta = z' - z$, after which (11) assumes the form

$$B_z(x, y, z) = B_z(z) \sin(nx - \omega t) \cos my, \quad (12)$$

where
$$B_z(z) = -\frac{\mu_0}{4\pi} \iiint \frac{j_x(z') \eta \sin m\eta \cos n\xi - j_y(z') \xi \sin n\xi \cos m\eta}{[\xi^2 + \eta^2 + \zeta^2]^{3/2}} d\xi d\eta dz'. \quad (13)$$

In (13) we carry out integration for ξ and η , using [12]:

$$\begin{aligned} \int_{-\infty}^{\infty} \int_{-\infty}^{\infty} \frac{\xi \sin n\xi \cos m\eta}{[\xi^2 + \eta^2 + \zeta^2]^{3/2}} d\xi d\eta &= \int_{-\infty}^{\infty} \xi \sin n\xi d\xi \int_{-\infty}^{\infty} \frac{\cos m\eta d\eta}{[\xi^2 + \eta^2 + \zeta^2]^{3/2}} = \\ &= \int_{-\infty}^{\infty} \xi \sin n\xi [2m/(\xi^2 + \zeta^2)^{3/2}] K_1(m\sqrt{\xi^2 + \zeta^2}) d\xi = \\ &= 4\sqrt{\pi}/2m(n^2 + m^2)^{-1/2} \zeta^{1/2} K_{-1/2}(\sqrt{n^2 + m^2} \zeta) = (2\pi n/k) e^{-n|\zeta|}, \end{aligned}$$

where $K_{1/2}(z)$, $K_{-1/2}(z)$ are cylindrical functions of a fictitious argument. The other integral is computed in a similar way:

$$\int_{-\infty}^{\infty} \int_{-\infty}^{\infty} \eta \sin m\eta \cos n\xi [\xi^2 + \eta^2 + \zeta^2]^{-3/2} d\xi d\eta = (2\pi m/k) e^{-n|\zeta|}.$$

As a result, formula (13) assumes the form:

$$B_z(z) = -(\mu_0/2) \int_0^{-z} [(m/k) j_x(z') - (n/k) j_y(z')] e^{-n|z'-z|} dz'. \quad (14)$$

Substituting into (14) the expressions for electric currents from (10), we obtain

$$\dot{B}_z(z) = -(\mu_0 n F / 2k) \int_0^{-z} \sigma(z') v(z', k) e^{-n|z'-z|} dz'. \quad (15)$$

As can be seen from (15), B_z is completely determined by wave velocity and the conductivity of sea water.

The horizontal components of magnetic induction B_x and B_y can be determined similar to B_z , but in a simpler approach. We will use equations (5) for magnetic induction: $\text{rot } B = \mu j$, $\text{div } B = 0$ and the fact that

$$B_x(x, y, z) = B_x(z) \cos(nx - \omega t) \cos my, \quad (16)$$

$$B_y(x, y, z) = B_y(z) \sin(nx - \omega t) \sin my,$$

and we obtain the equations

$$nB_y(z) + mB_x(z) = \mu j_z(z), \quad B_x'(z) + mB_y(z) - nB_x(z) = 0,$$

which lead to a determination of $B_x(z)$, $B_y(z)$:

FOR OFFICIAL USE ONLY

$$\begin{aligned} B_x(z) &= (\mu_0 m/k^2) j_z(z) + (n/k^2) B_z'(z), \\ B_y(z) &= (\mu_0 n/k^2) j_z(z) - (m/k^2) B_z'(z). \end{aligned} \quad (17)$$

In particular, $B_x(z)$ in the sea, that is, when $-H < z < 0$, is the following function of potential, velocity and conductivity:

$$\begin{aligned} B_x(z) &= -\frac{\mu_0 m}{k^2} \sigma(z) \varphi'(z) + e^{nz} \frac{\mu_0 n^2 F}{2k^2} \int_0^z \sigma(z') v(z') e^{-nz'} dz' - \\ &\quad - e^{-nz} \frac{\mu_0 n^2 F}{2k^2} \int_z^{-H} \sigma(z') v(z') e^{nz'} dz'. \end{aligned}$$

Electromagnetic fields in a sea with conductivity exponentially decreasing with depth. We will select the following model of the earth's electric conductivity: the atmosphere is dielectric, conductivity in the sea changes in conformity to the law

$$\sigma(z) = \sigma_{21} \exp(-2\alpha z), \quad (19)$$

where $\sigma(0) = \sigma_{21}$ is conductivity at the sea surface; $\sigma(-H) = \sigma_{22}$ is conductivity at the sea floor, the conductivity of the bottom is constant and equal to σ_3 . The α coefficient is determined by the ratio

$$\alpha = (2H)^{-1} \ln(\sigma_{22}/\sigma_{21}), \quad |\alpha| \sim H^{-1}.$$

We select a sea wave in the form (7), where $v(z, k) = v_0 \operatorname{sh} k(z + H)$, although it is also possible to select a potential sea wave, for example, a traveling progressive wave, which leads to the right-hand sides of the equations (6) and (8) becoming equal to zero. In accordance with the definition, $v(0, k) = v_0 \operatorname{sh} kH$ is the velocity at the sea surface, the maximum of all $v(z, k)$.

With the selected models of the wave and conductivity equation (8) in the sea assumes the form:

$$d^2\varphi(z, k)/dz^2 - 2\alpha d\varphi(z, k)/dz - k^2\varphi(z, k) = mFv_0 \operatorname{sh} k(z+H). \quad (20)$$

Equations (8) for the atmosphere ($z > 0$) and underlying bottom have an identical form:

$$d^2\varphi(z, k)/dz^2 - k^2\varphi(z, k) = 0 \quad (21)$$

We will denote by the subscripts 1, 2, 3 the fields and potentials in the atmosphere, sea and bottom respectively.

FOR OFFICIAL USE ONLY

Equations (20) and (21) in the corresponding media have the solutions:

$$\begin{aligned} \varphi_{1T}(z, k) &= C_{1T} e^{-kz}, \\ \varphi_{2T}(z, k) &= C_{2T} e^{(\alpha+\beta)z} + C_{3T} e^{(\alpha-\beta)z} - \frac{mFv_0}{2\alpha k} \operatorname{ch} k(z+H), \end{aligned} \quad (22)$$

$$\varphi_{3T}(z, k) = C_{4T} e^{kz},$$

where $\beta = \sqrt{\alpha^2 + k^2}$; $\gamma = \sigma_3 / \sigma_{22}$. The system of boundary conditions imposed on the potentials is

$$\begin{aligned} \varphi_{1T}(0) &= \varphi_{2T}(0), \quad \varphi_{2T}(-H) = \varphi_{3T}(-H), \\ d\varphi_{2T}(z)/dz|_{z=0} &= 0, \quad d\varphi_{2T}(z)/dz|_{z=-H} = \gamma d\varphi_{3T}(z)/dz|_{z=-H}, \end{aligned}$$

and makes it possible to find the coefficients $C_2\gamma$ and $C_3\gamma$:

$$C_{2T} = (S/\Delta_T) [e^{-(\alpha-\beta)H} (\gamma k - \alpha + \beta) \operatorname{sh} kH - \gamma (\alpha - \beta)], \quad (23)$$

$$C_{3T} = (S/\Delta_T) [e^{-(\alpha+\beta)H} (\alpha + \beta - \gamma k) + \gamma (\alpha + \beta)], \quad (24)$$

where

$$S = mFv_0/2\alpha k, \quad \Delta_T = e^{-\alpha H} [(k - \gamma\alpha) \operatorname{sh} \beta H + \gamma\beta \operatorname{ch} \beta H]. \quad (25)$$

The coefficients $C_1\gamma$ and $C_4\gamma$ are expressed through $C_2\gamma$ and $C_3\gamma$ in the following way:

$$\begin{aligned} C_{1T} &= C_{2T} + C_{3T} - S \operatorname{ch} kH, \\ C_{4T} &= C_{2T} e^{-(\alpha+\beta-k)H} + C_{3T} e^{-(\alpha-\beta-k)H} - S e^{\beta H}. \end{aligned}$$

For a nonconducting bottom $\gamma = 0$ and for the coefficients C_{20} and C_{30} from (23), (24) we obtain the following expressions with (25) taken into account:

$$\begin{aligned} C_{20} &= S [(\beta - \alpha) \operatorname{sh} kH / k \operatorname{sh} \beta H] e^{\beta H}, \\ C_{30} &= S [(\alpha + \beta) \operatorname{sh} kH / k \operatorname{sh} \beta H] e^{-\beta H}. \end{aligned} \quad (26)$$

If it is taken into account that the approximation which we have considered is a short-wave approximation, in formulas (23)-(26) it is possible to carry out simplifications, taking into account that in these expressions $kH \gg 1$ and $|\alpha| \sim H^{-1}$, and accordingly, $k \gg |\alpha|$, $\beta = k$, $\operatorname{sh} kH \approx \operatorname{ch} kH \approx e^{kH}/2$. We find

$$C_{2T} = S [(1+\gamma) e^{\beta H} + 2\gamma e^{\alpha H}] / (1+\gamma), \quad C_{3T} = S 2\gamma e^{\alpha H} / (1+\gamma), \quad (27)$$

$$C_{20} = S e^{\beta H}, \quad C_{30} = 0. \quad (28)$$

Then the approximate potential in the sea is determined by the expressions:

$$\begin{aligned} \bar{\varphi}_{2T}(z, k) &= \frac{S}{1+\gamma} \left\{ \left[e^{\alpha z} (1+\gamma) - \frac{1}{2} (1+\gamma) \right] e^{k(z+H)} + \gamma e^{\alpha(z+H)} \operatorname{ch} kz \right\}, \\ \bar{\varphi}_{30}(z, k) &= S (e^{\alpha z} - 1/2) e^{k(z+H)}. \end{aligned}$$

FOR OFFICIAL USE ONLY

Thus, for computation of the electric currents, electric field and magnetic induction field it is possible to use precise and approximate expressions for potential with the coefficients (23), (24) or (27) for a model with a conducting bottom and the coefficients (26) or (28) for a model with a dielectric bottom.

The vertical component of magnetic induction $B_z(z)$ is not dependent on the choice of a model of the bottom and can be computed using formula (15). We have:

$$B_z(z) = \frac{\mu_0 n F v_0 \sigma_{21}}{2k} \int_0^{-H} e^{-2\alpha r'} \operatorname{sh} k(z'+H) e^{-\lambda|z'-r'|} dz'.$$

This integral is broken down into two parts: in the first integration is carried out using the points z' of sources situated over the considered point, and we have $|z' - z| = z' - z$; in the second integration is carried out for the remaining region, that is, using the points over the considered point, and we have $|z' - z| = z - z'$. For the vertical component of magnetic induction in the water we obtain

$$B_z(z) = B_0 \frac{n}{k} \left\{ \frac{1}{2\alpha} [e^{\lambda(r+H)} (1 - e^{-2\alpha z}) - e^{-\lambda(z+H)} (e^{2\alpha H} - e^{-2\alpha z})] + \frac{1}{2(\alpha+k)} e^{-\lambda H} (e^{-(2\alpha+k)r} - e^{\lambda r}) - \frac{1}{2(\alpha-k)} e^{\lambda(H-r)} (e^{2(\alpha-k)H} - e^{-2(\alpha-k)r}) \right\},$$

where $B_0 = \mu_0 v_0 F \sigma_{21}/4$.

A numerical estimate of B_z at the sea surface, that is, with $z = 0$ and with the following values of the parameters: $k \approx 0.03 \text{ m}^{-1}$, $H = 10^3 \text{ m}$, $v_0 \operatorname{sh} kH = 1 \text{ m/sec}$, $\sigma_{21} = 5 \text{ Cm}$, gives $B_z(0) \approx 1.2 \text{ nT}$.

The tangential components of the magnetic induction field are found using formulas (17), (18). It is easy to determine the components of the electric field using formulas (9) and the components of the electric current using formulas (10).

In conclusion it should be noted that the use of the exponentially decreasing function (19) for electric conductivity of the sea with depth with the coefficients $|\alpha| \sim H^{-1}$ does not ensure the required marked decrease in conductivity, especially at depths to 1,000 m, which, on the one hand, makes it necessary to seek the functions most precisely approximating the experimental variation of electric conductivity, and on the other hand, use a multilayer electrically stratified model of the ocean.

Another important direction in the work should be related to solution of equations (3) and (4), making it possible to include electromagnetic fields of medium- and long-period waves in the system of computations.

FOR OFFICIAL USE ONLY

FOR OFFICIAL USE ONLY

BIBLIOGRAPHY

1. Trayman, R., GEOMAGNETIZM I AERONOMIYA (Geomagnetism and Aeronomy), 10, 478, 1970.
2. ELECTROMAGNETIC PROBING IN GEOPHYSICS, edited by J. R. Wait, The Golem Press, Boulder, Colorado, 1971.
3. Cox, C. S., Fillouz, J. H., Larson, J. C., THE SEA, Vol 4, 1, 637, Wiley-Interscience, New York, 1971.
4. Bullard, E. C., Parker, R. L., THE SEA, Vol 4, 1, 695, Wiley-Interscience, New York, 1971.
5. Fonarev, G. A., Shneyer, V. S., MORSKIYE TOKI (Sea Electric Currents), GEOMAGNETIZM I VYSOKIYE SLOI ATMOSFERI (Geomagnetism and High Layers of the Atmosphere), No 2, "Nauka," 225, 1975.
6. Sanford, T. B., JGR, 76, 3476, 1971.
7. Larsen, J. C., PHYS. EARTH AND PLANET. INTER., 7, 389, 1973.
8. Landau, L. D., Lifshits, Ye. M., ELEKTRODINAMIKA SPLOSHNYKH SRED (Electrodynamics of Continuous Media), Chapter VIII, Gostekhizdat, 1957.
9. Warburton, R., Caminiti, R., JGR, 69, 4311, 1964.
10. Leybo, A. B., Semenov, V. Yu., GEOMAGNETIZM I AERONOMIYA, 15, 236, 1975.
11. Leybo, A. B., Semenov, V. Yu., Fonarev, G. A., GEOMAGNETIZM I ISSLEDOVANIYA (Geomagnetic Research), No 16, "Nauka," 30, 1975.
12. Gradshteyn, I. S., Ryzhik, I. M., TABLITSY INTEGRALOV, SUMM, RYADOV I PROIZVEDENIY (Tables of Integrals, Sums, Series and Products), Fizmatgiz, 1963.

COPYRIGHT: Izdatel'stvo "Nauka," "Geomagnetizm i aeronomiya," 1979

[495-5303]

FOR OFFICIAL USE ONLY

FOR OFFICIAL USE ONLY

UDC 551.46.01

SYSTEMIC PRINCIPLES FOR ANALYSIS OF OCEAN OBSERVATIONS

Kiev SISTEMNYYE PRINTSIPY ANALIZA NABLYUDENIY V OKEANE (Systemic Principles for Analysis of Ocean Observations) in Russian 1978 pp 2-3, 221-222

[Annotation, introduction and table of contents from book by B. A. Nelepo and I. Ye. Timchenko, Izdatel'stvo "Naukova Dumka," 224 pages]

[Text] This monograph is devoted to a systemic approach to the problem of predicting oceanic phenomena by means of automation of the data collection and processing processes. On the basis of the theory of adaptive filtering of observations the monograph examines dynamic-stochastic models of processes and fields in the ocean and validates the principles for combining hydrodynamic problems in oceanography with statistical methods for the analysis of observations. As component parts of the systemic approach, a study is made of problems in the optimum interpolation of random fields and the planning of measurements in the ocean.

The authors give examples of the use of dynamic-stochastic models for the successive prediction of oceanic processes and fields. The monograph is intended for professional geophysicists working on the problems of modeling and numerical analysis of physical processes and fields.

Sixty-nine illustrations. Five tables. Bibliography (pp 213-220) 193 items.

Introduction. Prediction of the state of the ocean as a medium is of great scientific and practical importance for mankind. The knowledge accumulated by oceanology is evidence of the complex spatial-temporal variability of the principal hydrophysical, hydrochemical and biological fields in the ocean. As a result of the infinite diversity of the factors forming weather in the ocean, in addition to the equations of hydromechanics, describing the principal features of the dynamics of water masses, use is made of different stochastic methods for the modeling and filtering of observational data. The problems arising with a combination of determined and stochastic approaches to the investigation of oceanic phenomena remain virtually unstudied. However, under conditions of automation of collection and processing of

FOR OFFICIAL USE ONLY

FOR OFFICIAL USE ONLY

oceanological data such a research method (which we have arbitrarily called the systemic approach to the analysis of a phenomenon) should be most effective. This monograph is devoted to use of the systemic approach in the problems involved in computing and predicting oceanological processes and fields on the basis of observational data.

Due to the poor study of most of the considered matters, the book gives no review of oceanological studies of stochastic modeling and analysis of oceanic fields. Problems in objective and four-dimensional analyses of meteorological fields, similar in formulation, have been dealt with only to the extent which was deemed necessary, taking into account their specific nature. Individual results of this study (for example, possible variants of oceanological data systems) must be regarded only as a formulation of the problem for further investigation.

We consider it our pleasant duty to express deep appreciation to Academicians L. M. Brekhovskikh and A. M. Obukhov and Corresponding Member USSR Academy of Sciences A. S. Monin for discussion of individual parts of the study and valuable advice favoring an improvement in its content.

Contents	Page
Introduction	3
Chapter I. Problems in Physics of the Ocean and Modern Systems Theory	4
1. Applied aspects of oceanological research	4
2. Automation of processes of collection and processing of oceanological information	9
3. Systems approach to analysis of oceanic phenomena	16
4. Problem of prediction and filtering of processes and fields in the ocean	22
5. General principles for planning ocean observations	31
Chapter II. Optimum Filtering of Observations of Random Oceanological Processes	37
6. Optimum filtering of observation time series as a problem in control theory	37
7. Algorithm for the optimum filtering of time series of oceanological observations	45
8. Identification of parameters of models of stationary hydrophysical processes	48
9. Prediction of stationary hydrophysical processes by Kalman method	53
10. Modeling of nonstationary hydrophysical processes	60
11. Automation of modeling and prediction, on an electronic computer, of nonstationary hydrophysical processes	67
Chapter III. Objective Analysis of Spatial Random Ocean Fields	74
12. Statistical modeling of spatial random ocean fields	74
13. Optimum interpolation correlation algorithm	78
14. Construction of maps of hydrophysical fields by optimum interpolation method	31

FOR OFFICIAL USE ONLY

15. Construction of maps of spatial distribution of oxygen based on observations in the Tropical Atlantic	85
16. Spectral optimum interpolation algorithm	96
17. Use of spectral interpolation algorithm in problems of construction of maps of ocean fields	106
18. Statistical matching of oceanographic fields	113
19. Refinement of map of oxygen field on basis of measurements of the salinity field	122
Chapter IV. Sequential Methods for Predicting Ocean Fields	128
20. Use of methods for four-dimensional analysis of observations in meteorology	128
21. Formulation of problem of successive analysis of spatial-temporal ocean fields	134
22. Spectral formulation of successive analysis method	141
23. Properties of algorithm for successive analysis of observations	143
24. Successive analysis of observations of vertical distribution of current velocities	147
25. Prediction of vertical temperature profiles in upper layer of sea	156
26. Modeling and prediction of the vertical distribution of sea temperature under expeditionary conditions	164
Chapter V. Systemic Approach to Planning of Oceanographic Observations	174
27. Measurement of oceanographic processes in relation to use of adaptive filtering methods	174
28. Planning of network of stations for measuring random spatial oceanic fields	176
29. Rationalization of survey of spatial field of bottom relief	190
30. Measurement of statistically related fields	195
31. Planning of observations of spatial-temporal fields in ocean	199
32. Organization of collection and processing of data in successive analysis of oceanographic information	207
Bibliography	213

COPYRIGHT: Izdatel'stvo "Naukova dumka," 1978

5303
CSO: 1866

-END-